

**Figure 17.1**

Shape defined in relation to the circular form.

Shape factors of four non-circular shapes are shown schematically.

(a) Circle = reference shape: isometric, fully convex, continuously curved;

(b) square: isometric ( $a / b = 1.00$ ), fully convex, angular;

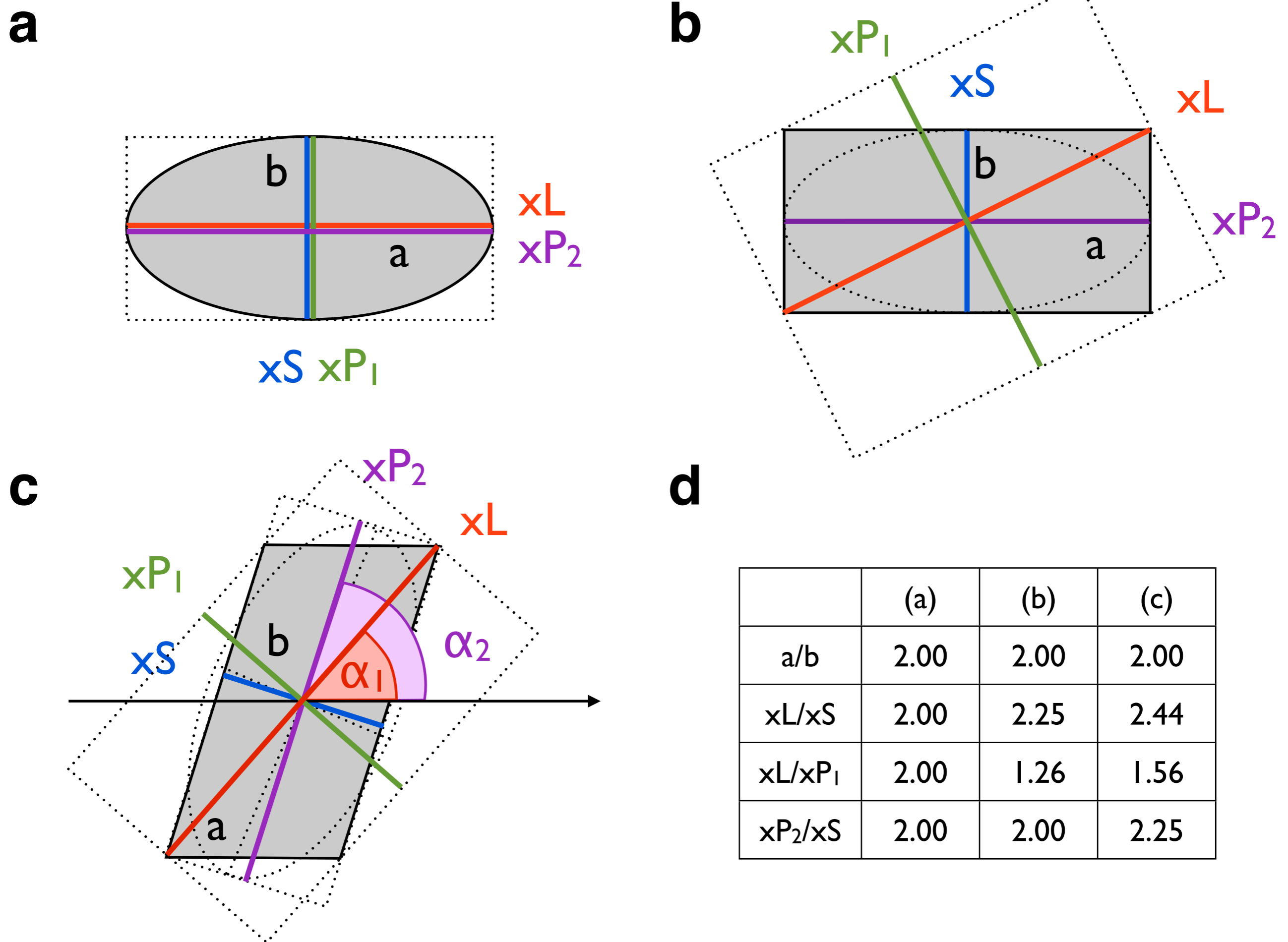
(c) ellipse: elongated ( $a / b > 1.00$ ), fully convex, continuously curved;

(d) lobate shape; isometric, convex-concave, continuously curved;

(e) angular fragment: isometric, convex-concave, angular;

shape factors:  $SF_1 =$  perimeter ratio  $P / P_{equ}$ ;  $SF_2 =$  area ratio  $4\pi A / P^2$ ;

$A =$  measured area of shape;  $P =$  measured length of outline;  $P_{equ} =$  perimeter of area equivalent circle.



**Figure 17.2**

Defining long and short axes.

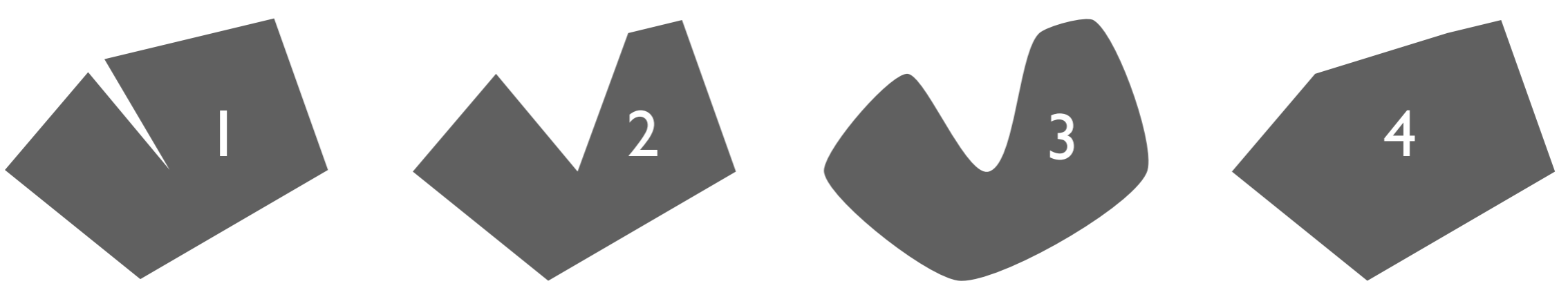
See chapter 14 for PAROR method. Long and short axes derived from projections are shown for an ellipse (a), a rectangle (b) and a parallelogram (c); stippled ellipses are best-fit ellipses; (d) table of values; stippled rectangles are bounding boxes for different long and short axes.

a = long axis; b = short axis of best-fit ellipse;

xS = shortest projection, xL = longest projection;

xP<sub>1</sub> = projection at 90° to xL ('perpendicular to long'); xP<sub>2</sub> = projection at 90° to xS ('perpendicular to short');

α<sub>1</sub> = orientation of xL; α<sub>2</sub> = orientation of xP<sub>2</sub>.



#	SF <sub>1</sub>	SF <sub>2</sub>	a / b shape	a / b rectangle	a / b ellipse	L / S shape	L / S rectangle	L / S ellipse
1	1.48	0.46	1.5	4.6	4.9	1.6	4.7	4.9
2	1.48	0.46	1.7	4.6	4.9	1.6	4.7	4.9
3	1.41	0.50	1.6	4.0	4.4	1.6	4.1	4.4
4	1.18	0.72	1.4	1.9	2.7	1.6	2.2	2.7



**Figure 17.3**

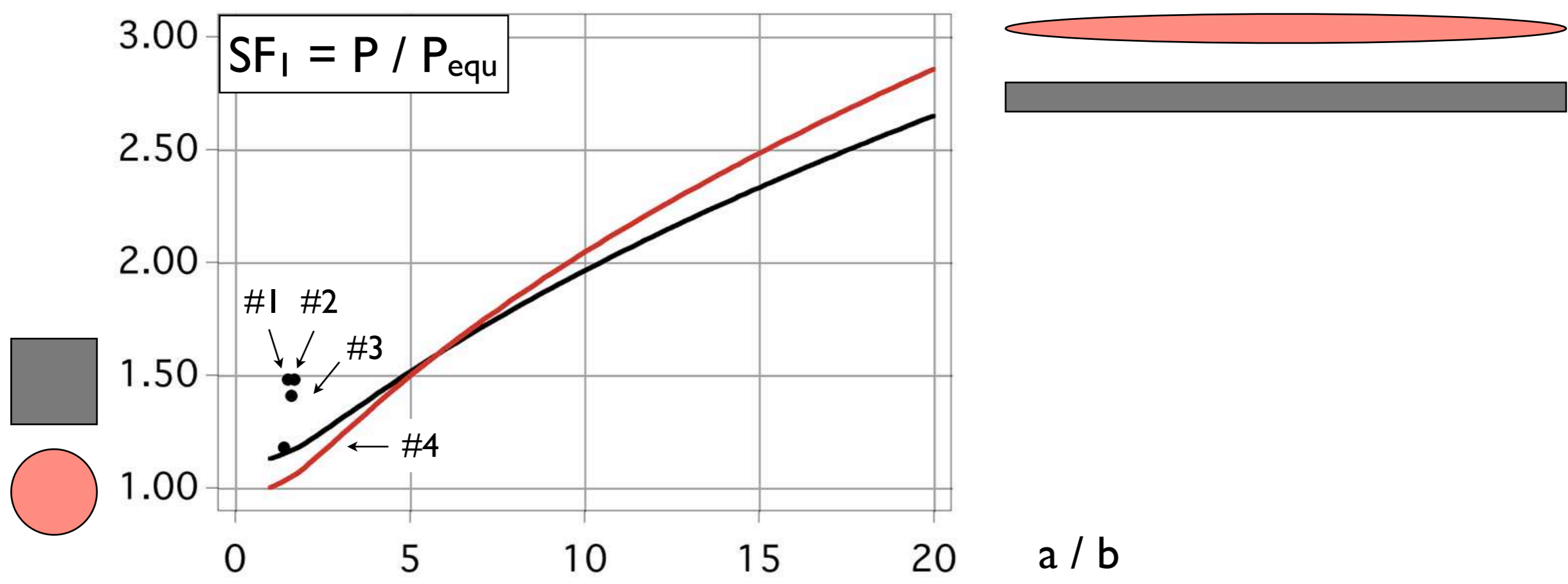
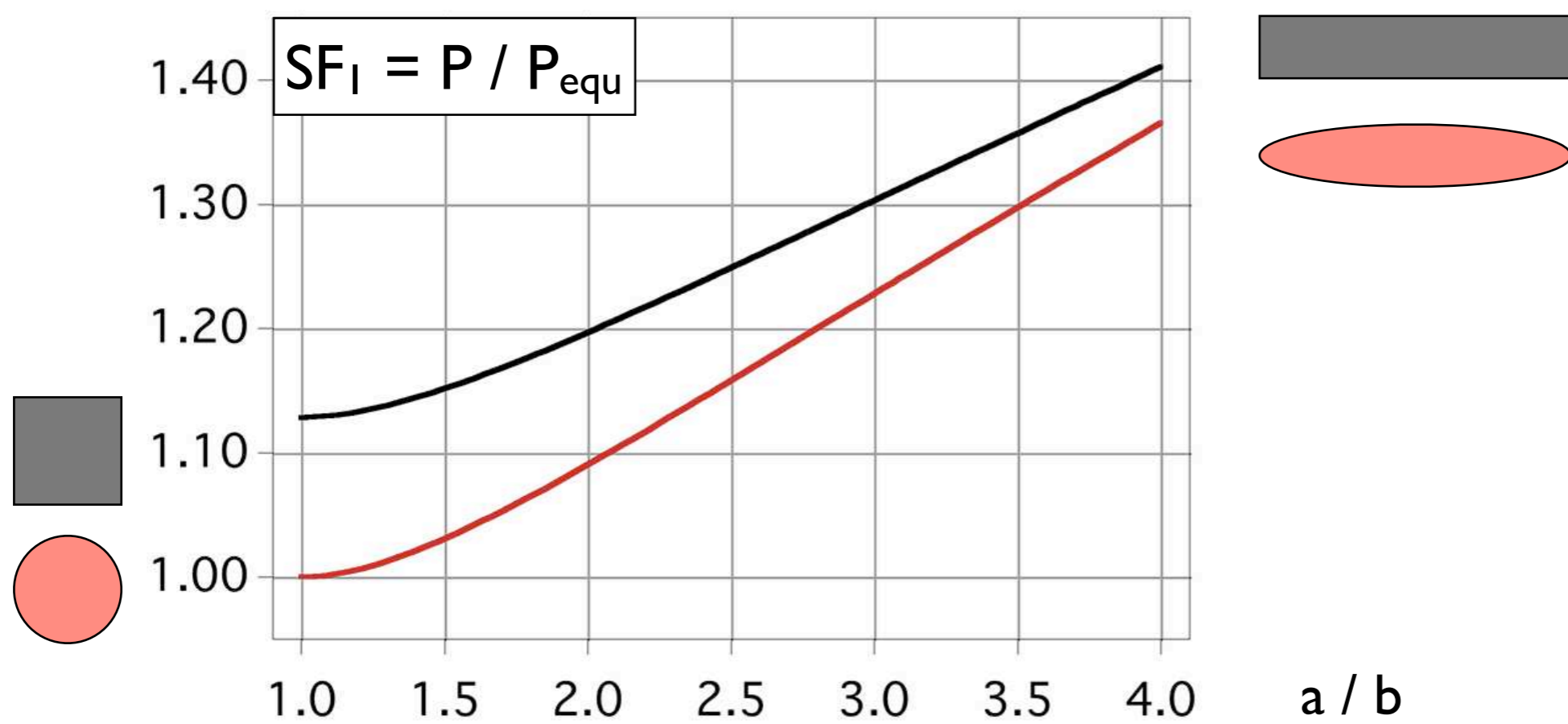
Shape factors of 4 test shapes.

$SF_1 = P / P_{equ}$ ;  $SF_2 = 4\pi \cdot A / P^2 = 1 / (SF_1)^2$ , where  $P$  = measured perimeter,  $P_{equ}$  = perimeter of area equivalent circle,  $A$  = measured area;

$a / b$  = aspect ratio derived from best-fit ellipse;

$L / S$  = aspect ratio derived from longest and shortest projection;

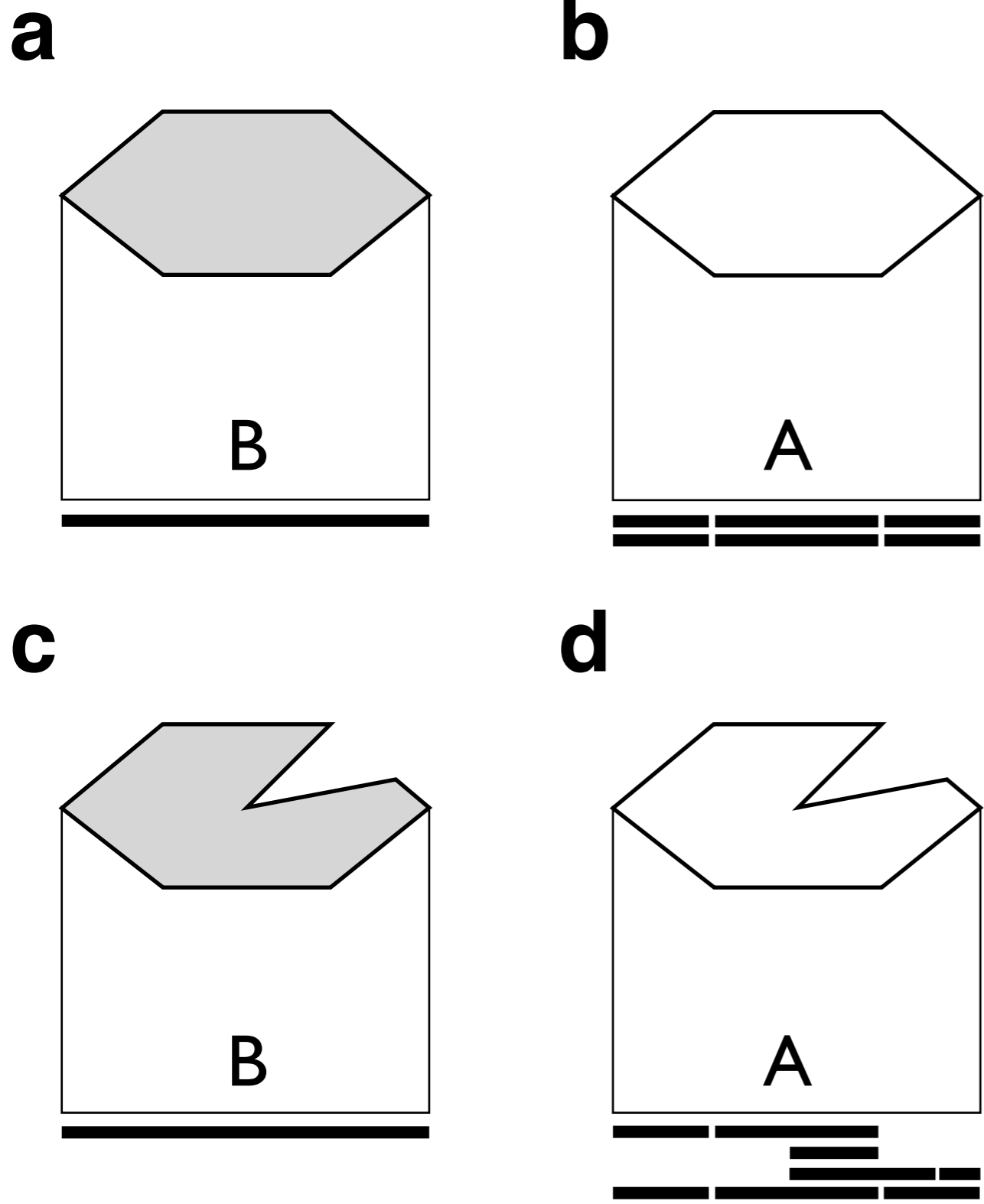
four rectangles and four ellipses with same shape factors as test shapes are shown for comparison.

**a****b****Figure 17.4**

Shape factors as a function of elongation.

(a) Shape factor  $SF_I = \text{perimeter ratio } P / P_{equ}$  is shown for ellipses (red curve) and rectangles (black curve) with increasing aspect ratio  $a / b$ ; dots indicate the shape factors of shapes in Figure 17.3;

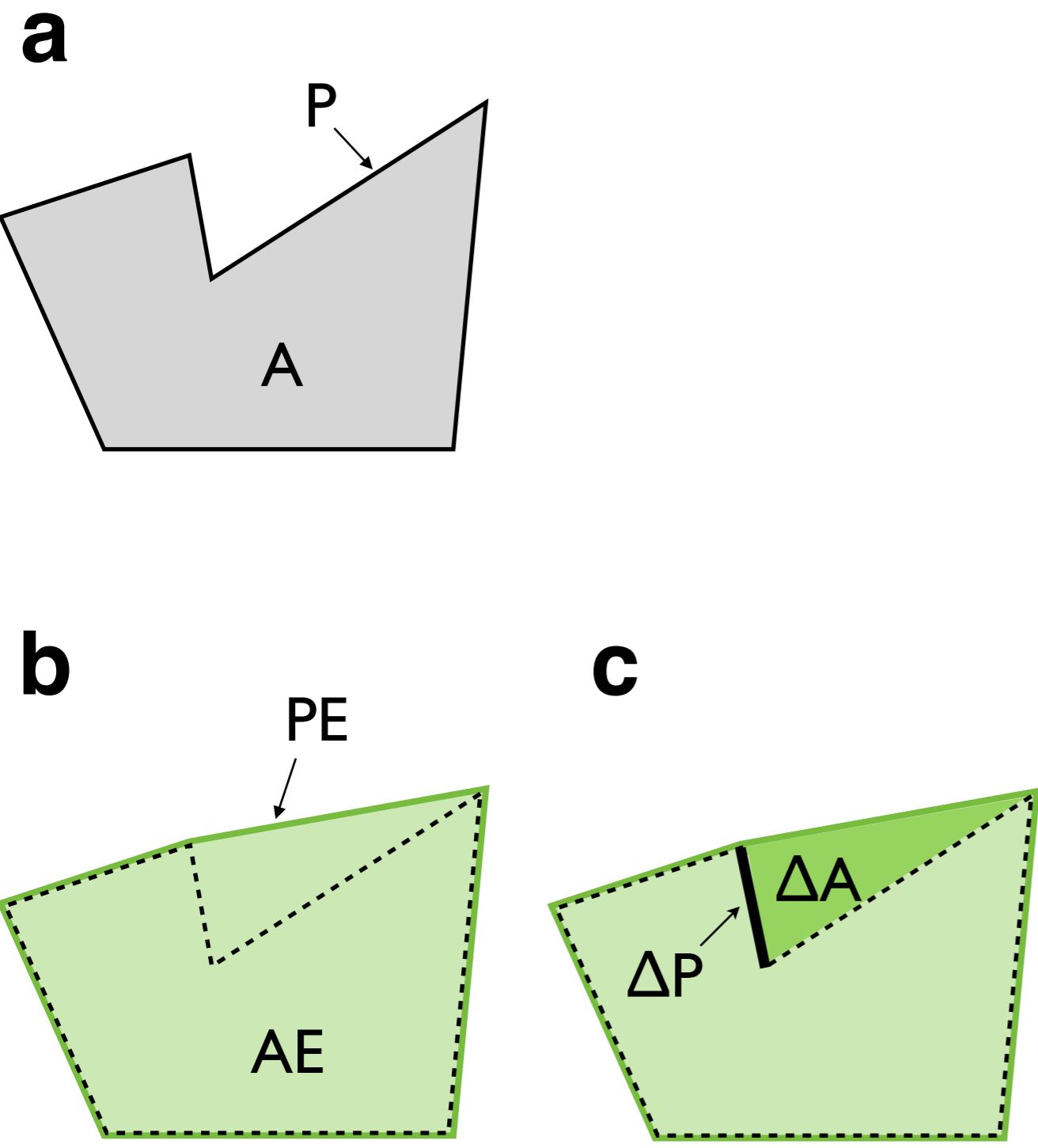
(b) detail of plot (a).



**Figure 17.5**

Projection of convex and concave outlines.

- (a) Particle projection, B, of a fully convex shape; (compare PAROR, chapter 14);
- (b) surface projection, A, of the same shape as (a) (compare SURFOR, chapter 15);
- (c) particle projection, B, of convex-concave shape;
- (d) surface projection, A, of same shape as (c).



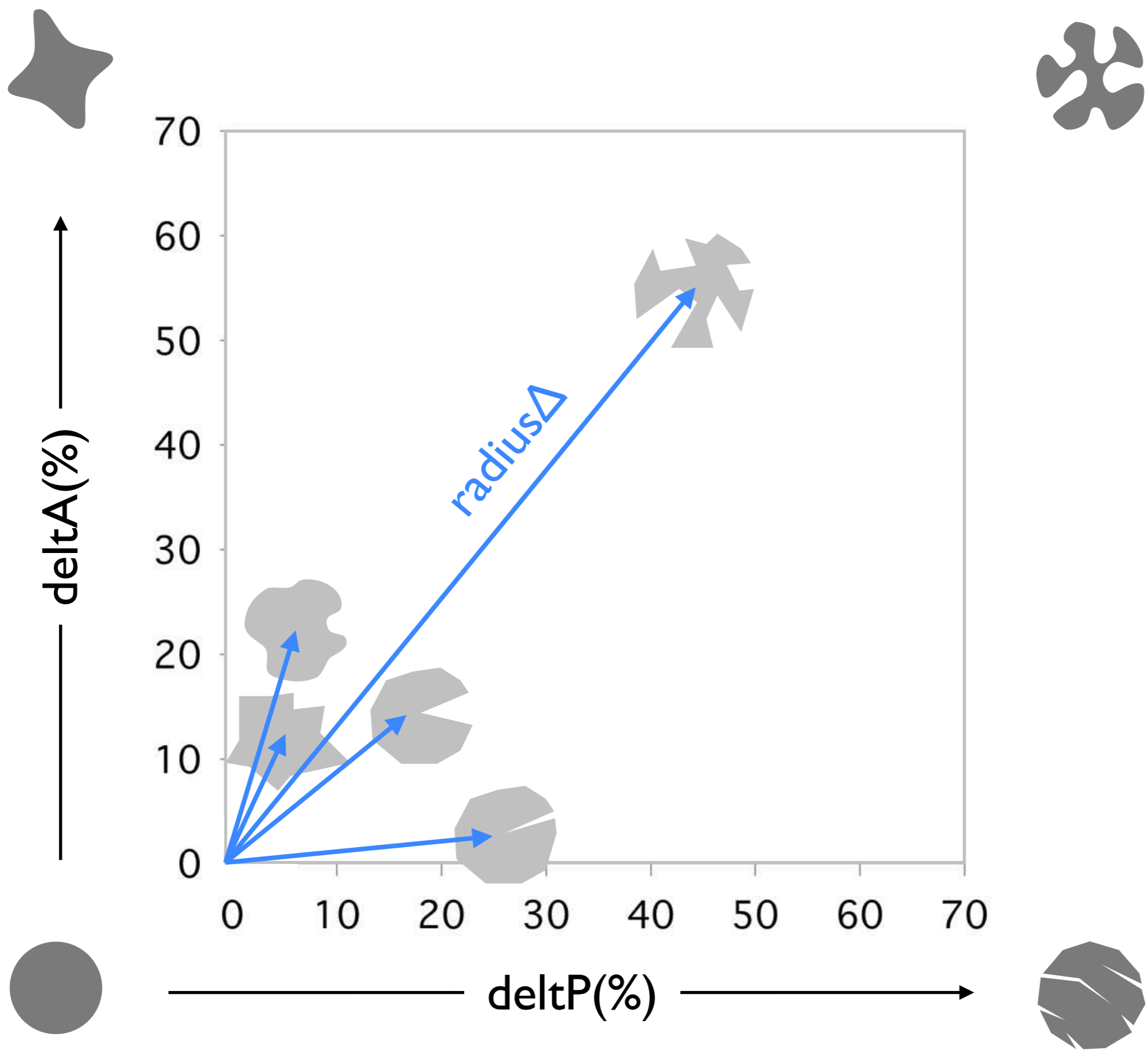
**Figure 17.6**

Shape factors derived from the convex hull.

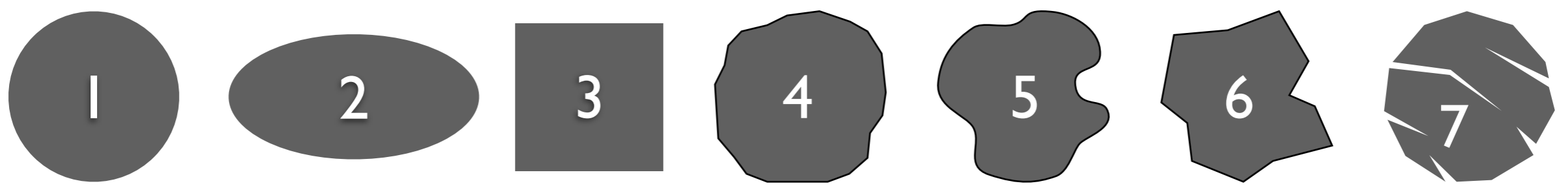
(a) Convex-concave shape with area,  $A$ , and perimeter,  $P$ ;

(b) convex hull around shape (a) with area,  $AE$ , and perimeter,  $PE$ ;

(c) heavy black line = excess perimeter,  $\Delta P = P - PE$ ; dark green = defect area,  $\Delta A = AE - A$ .



**Figure 17.7**  
Combining two shape factors.  
Plot of delta A (defect area) versus delta P (excess perimeter);  
radiusDelta (radius length) =  $\sqrt{(\text{delta P}^2 + \text{delta A}^2)}$ .



#	SF <sub>1</sub>	SF <sub>2</sub>	PARIS (%)	deltP (%)	deltA (%)	radiusΔ (%)
1	1.00	1.000	0	0	0	0.0
2	1.15	0.761	0	0	0	0.0
3	1.12	0.791	0	0	0	0.0
4	1.07	0.871	1.1	0.5	1.2	1.3
5	1.20	0.695	14.6	6.8	9.3	11.5
6	1.25	0.645	10.4	4.9	11	12.0
7	2.12	0.223	192.4	49	6.6	49.5

**Figure 17.8**

Comparison of shape descriptors for convex-concave forms.

$SF_1 = P / P_{equ}$ ;

$SF_2 = 4\pi \cdot A / P^2 = 1 / (SF_1)^2$ ;

$deltP = \text{excess perimeter} = (P-PE) / P$ ;



























$deltA = \text{defect area} = (AE-A) / A$ ;

$PARIS = \text{Percentile Average Relative Indented Surface} = 2 \cdot (P-PE) / PE \cdot (P-PE) / PE$ ;

$radius\Delta = \sqrt{(deltP^2 + deltA^2)}$ ;

P = measured perimeter, P<sub>equ</sub> = perimeter of area equivalent circle, A = measured area; PE = perimeter of convex hull; AE = area of convex hull.



rank	1.	2.	3.	4.	5.	6.	7.	
	weakest			←————→				strongest
SF <sub>1</sub>								
PARIS	  							
deltP								
deltA								
radiusΔ								

**Figure 17.9**

Ranking of shapes by different shape descriptors.

SF<sub>1</sub>: increasing deviation from circular form ('non-circularity');

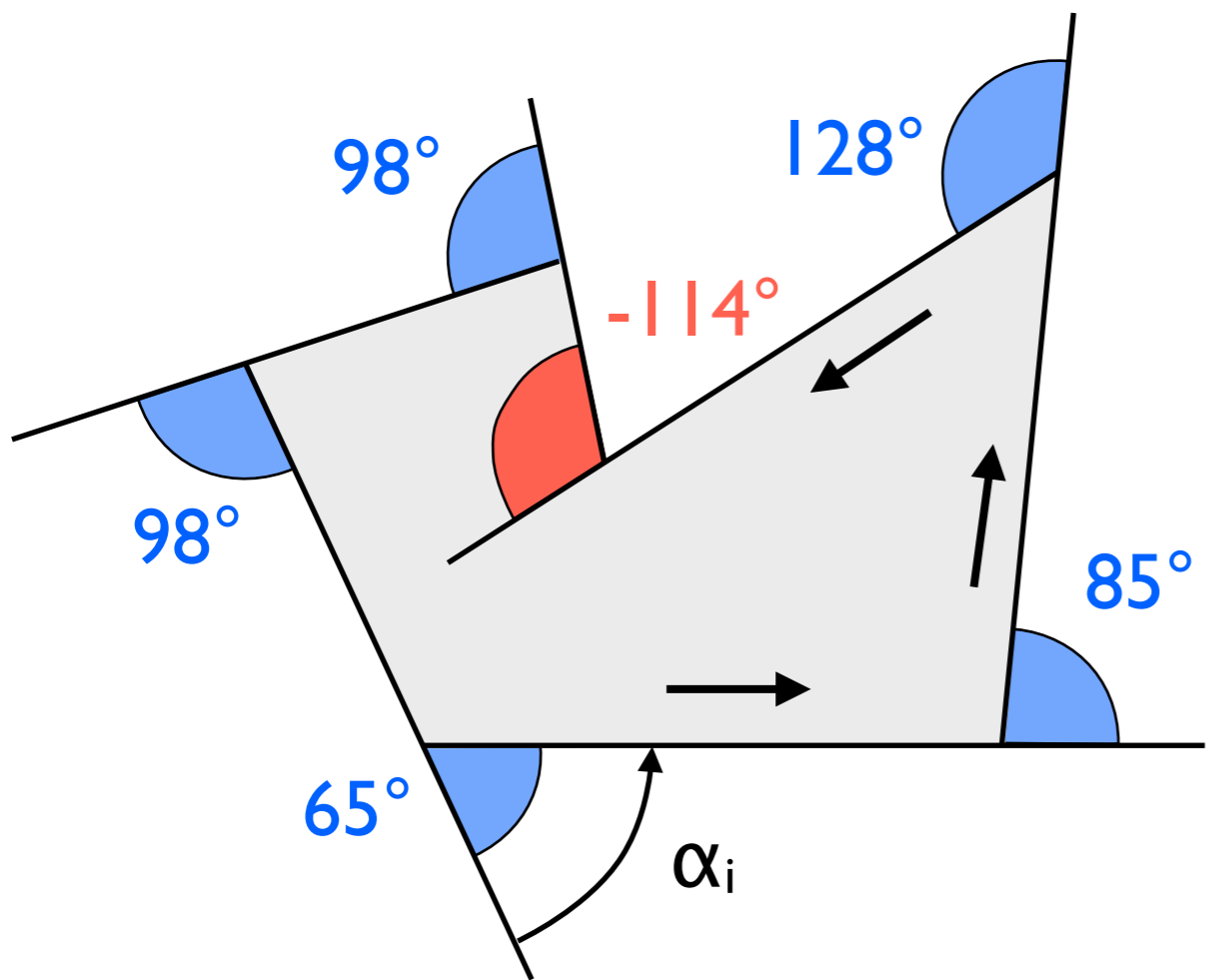
PARIS factor: increasing fraction of concave outline;

deltP: increasing fraction of concave outline;

deltA: increasing fraction of concave area;

radiusΔ: increasing fraction of concave outline and area;

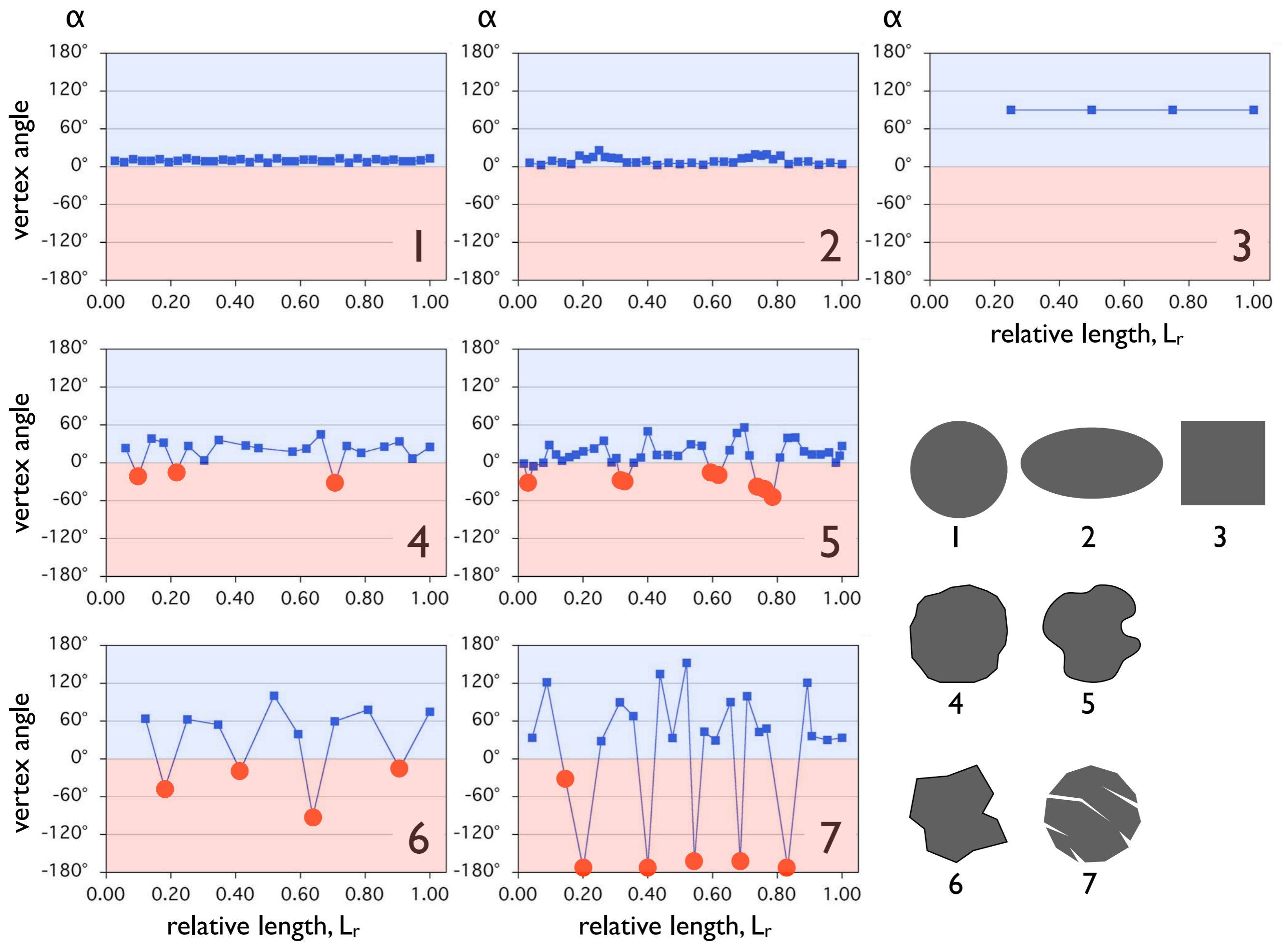
light gray shapes indicate that circle, square and ellipse cannot be ranked, PARIS, deltP, deltA and radiusΔ are identical = 0%.



**Figure 17.10**

Vertex angles of polygon.

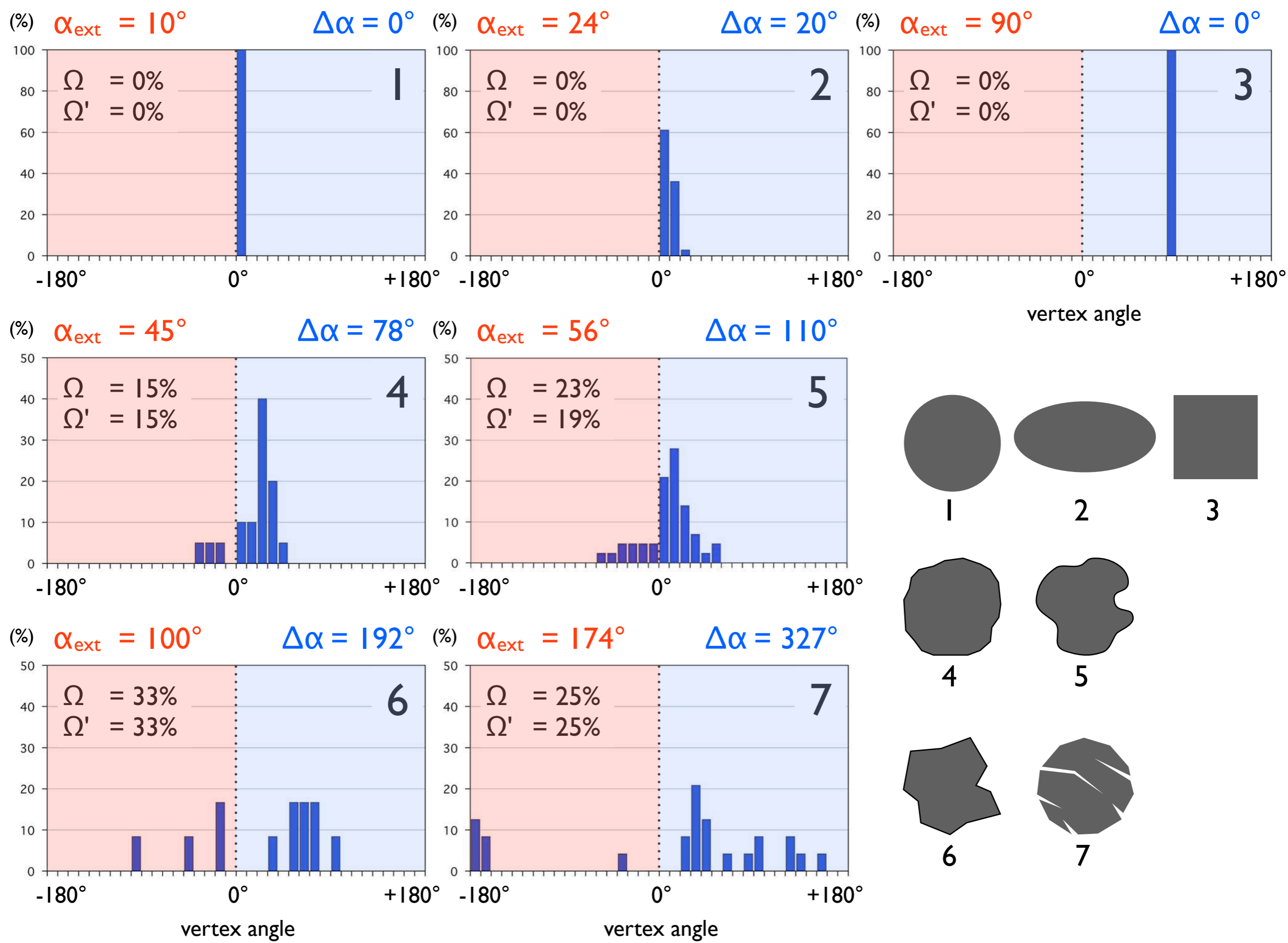
Polygonal chain (black outline) is shown with a counterclockwise loop (arrows); vertex angles,  $\alpha_i > 0^\circ$  (blue) if rotation is in the sense of closing (convex corner),  $\alpha_i < 0^\circ$  (red) if rotation is in the sense of opening (concave corner); for any polygon  $\sum \alpha_i = 360^\circ$ .



**Figure 17.11**

Vertex angles of test shapes.

Angles,  $\alpha_i$ , are plotted against relative length of outlines ( $0 \leq L_r \leq 1.00$ ); blue = positive (convex), red = negative (concave).



**Figure 17.12**

Histograms of vertex angles.

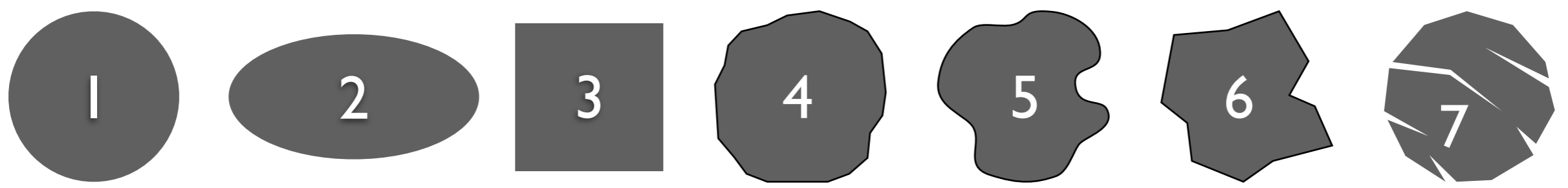
Frequencies are shown up to 100% for shapes 1 to 3, and up to 50% for shapes 4 to 7, positive values of vertex angles,  $\alpha_i$ , (convex corners) are highlighted in blue, negative values (concave corners) are highlighted in red;

$\Omega$  = sum of frequencies from  $-180^\circ$  to  $0^\circ$ ;

$\Omega'$  = sum of frequencies from  $-180^\circ$  to  $-10^\circ$ ;

$\alpha_{\text{ext}}$  = value of maximum absolute vertex angle;

$\Delta\alpha = \alpha_{\text{max}} - \alpha_{\text{min}}$ .



#	$\Omega$ (%)	$\Omega'$ (%)	$\alpha_{\text{ext}}$ (°)	$\Delta\alpha$	$\sigma\alpha$
1	0	0	10	0	0
2	0	0	24	20	6
3	0	0	90	0	0
4	15	15	45	78	20
5	23	19	56	110	24
6	33	33	100	192	59
7	25	25	174	327	105

**Figure 17.13**

Comparison of shape descriptors for angular forms.

$P$  = measured perimeter,  $P_{\text{equ}}$  = perimeter of area equivalent circle,  $A$  = measured area;  $PE$  = perimeter of convex hull;  $AE$  = area of convex hull;



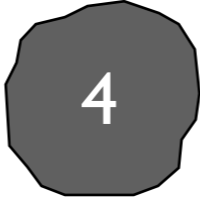















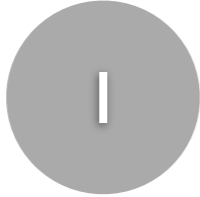












$\Omega$  = sum of frequencies form  $-180^\circ$  to  $0^\circ$ ;

$\Omega'$  = sum of frequencies form  $-180^\circ$  to  $-10^\circ$ ;

$\alpha_{\text{ext}}$  = value of maximum absolute vertex angle;

$\Delta\alpha$  =  $\alpha_{\text{max}} - \alpha_{\text{min}}$ ;

$\sigma\alpha$  = standard deviation of vertex angles.

rank	1.	2.	3.	4.	5.	6.	7.
	weakest			←————→			strongest
$\Omega$							
$\Omega'$							
$\alpha_{\text{ext}}$							
$\Delta\alpha$							
$\sigma_{\alpha}$							

**Figure 17.14**

Ranking of shapes by different descriptors for angularity.

$\Omega$  = sum of frequencies from  $-180^\circ$  to  $0^\circ$ ;

$\Omega'$  = sum of frequencies from  $-180^\circ$  to  $-10^\circ$ ;

$\alpha_{\text{ext}}$  = value of maximum absolute vertex angle.

$\Delta\alpha$  =  $\alpha_{\text{max}} - \alpha_{\text{min}}$ ;

$\sigma_{\alpha}$  = standard deviation of vertex angles;

light gray shapes indicate that shapes cannot be ranked:  $\Omega$  and  $\Omega'$  of circle, square and ellipse are identical = 0%;  $\Delta\alpha$  and  $\sigma_{\alpha}$  of the circle and the square are identical =  $0^\circ$ .

-----  
\*\*\* ishapes \*\*\*

2012-02-28, rh  
-----

calculates shape factors and angles of polygons  
(open outlines are closed)  
deltP=(PE-P)/P (≠PARIS)  
deltA=(AE-A)/A  
prints results on screen and in files  
minimum number of points per particles = 3  
maximum number of points per particles = 4000  
number of particles is unlimited...

-----  
input file:

```
line 1:          bti          title (must have)
line 2:          n            total number of points
for each particle: x,y        floating x-y coordinates
|                  ...          ...etc.
|                  Xend,Yend    end coordinates
```

-----  
name of input file:

**1** gouge.scm  
end coordinate of input file (0, 9999, ... one number):

**2** 9999

want results on screen (0), in files (1), or both (2):

**3** 2

**4** name of output file (angles) ? [gouge.scm.ang] (=default) >

**5** name of output file (shapes) ? [gouge.scm.shp] (=default) >

**6** name of output file (envelopes) ? [gouge.scm.elp](=default) >

-----  
results:

-----  
#    n(in) n(out)    S/L       L/p       phiL       paris       deltP       delTA  
  1    18    18       0.607       1.625       170.       1.05       0.53       2.45  
  2    13    13       0.776       1.167       140.       2.17       1.07       2.69  
  3     9     9       0.825       1.077       3.       0.00       0.00       0.00  
  ...  
 13    10    10       0.548       1.651       35.       1.27       0.64       2.63  
 14     8     8       0.833       1.074       54.       0.00       0.00       0.00

file with 14 grains ( 177 points) evaluated  
-----

output files:

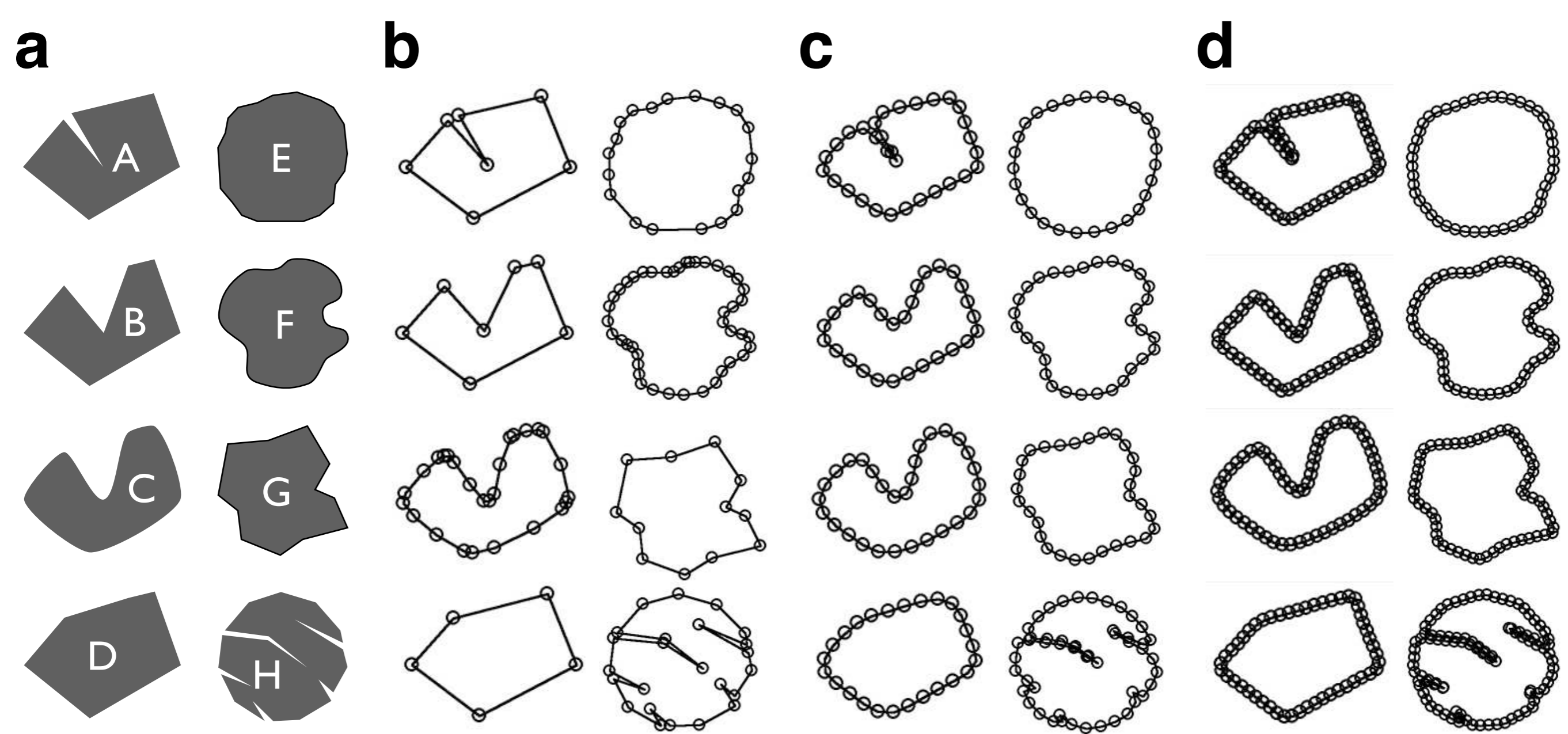
- gouge.txt.scm.ang
- gouge.txt.scm.shp
- gouge.txt.scm.elp

-----  
(screen output is not saved)

### Software Box 17.1

Dialog with program iSHAPES; answers are numbered and highlighted, see text for explanation.





**Figure 17.15**

Manual and automatic digitization of test shapes.

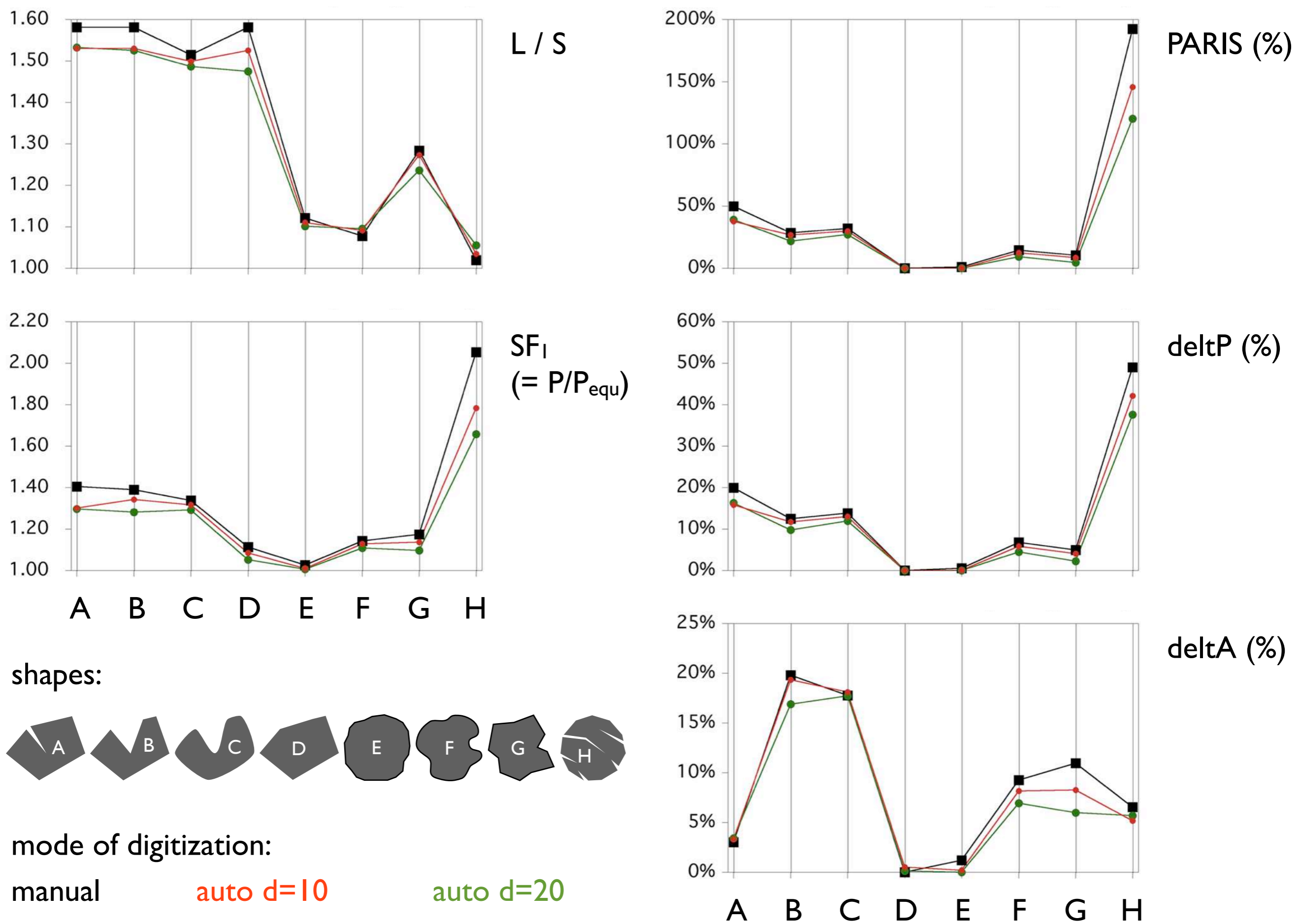
Previously used test shapes are digitized and represented by polygonal chains:

(a) manually digitized outlines (polygonal chains);

(b) automatically digitized outlines, minimal distance between points = 20 pixels, smoothing error = 1 pixel;

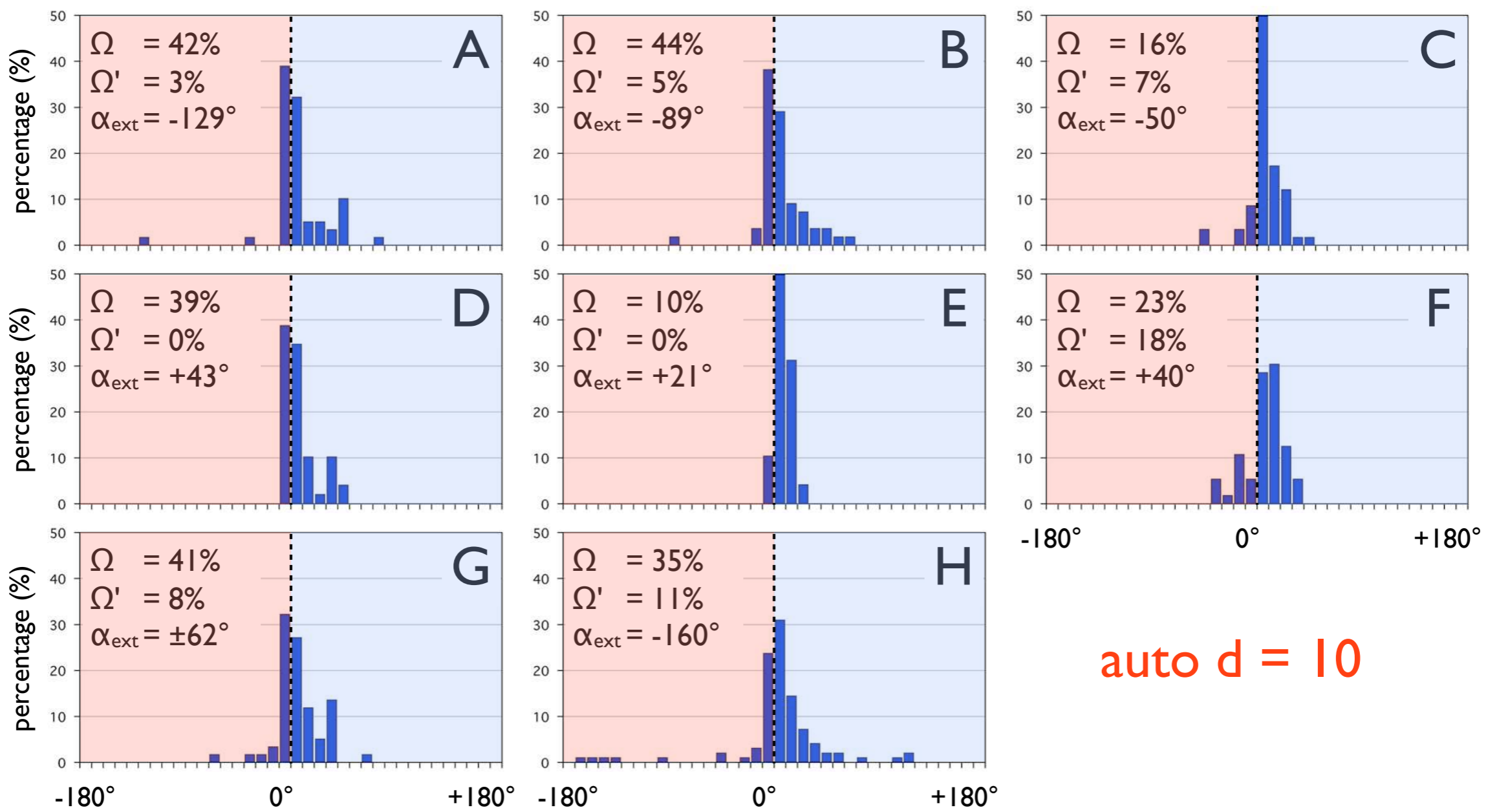
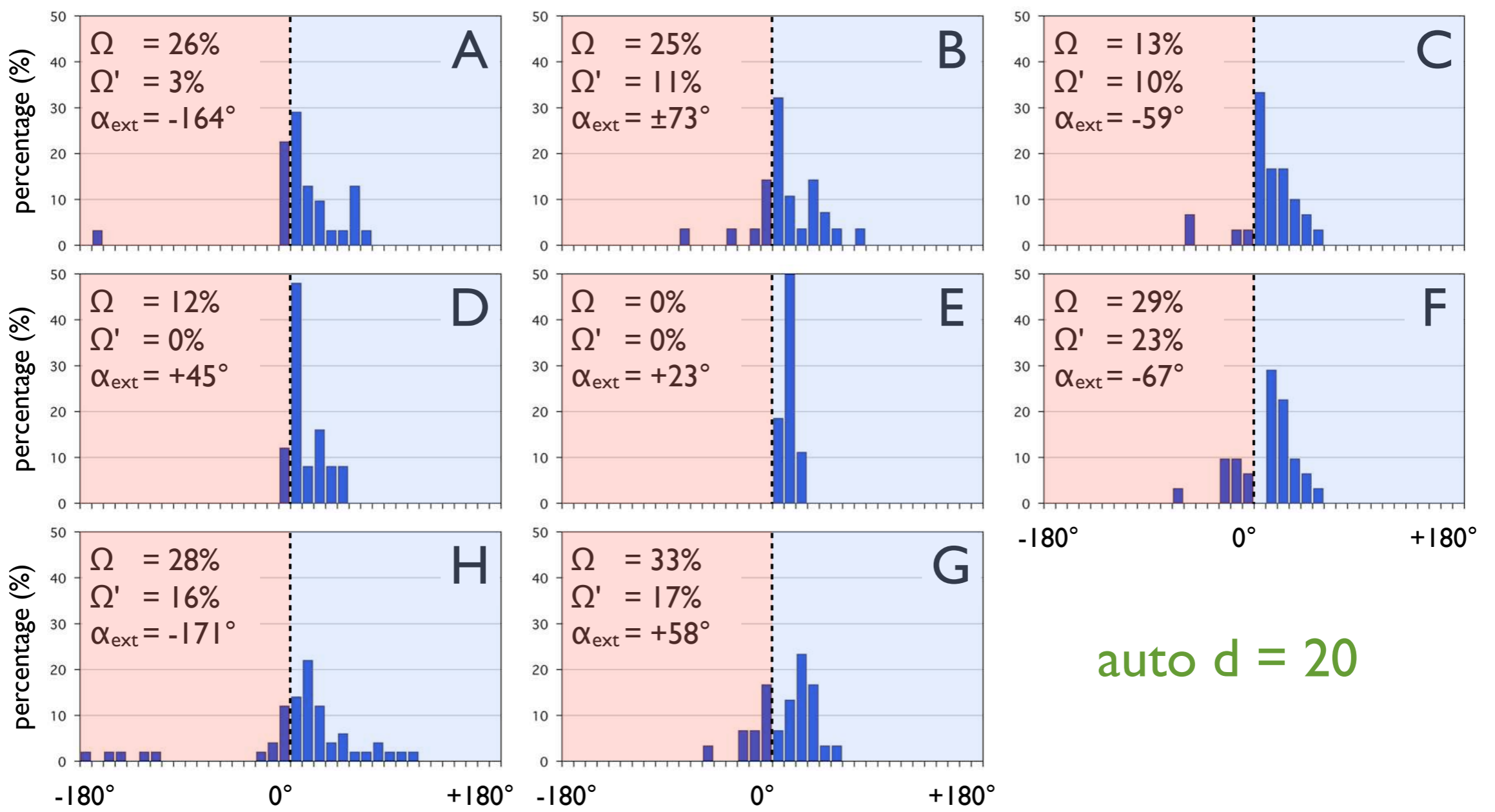
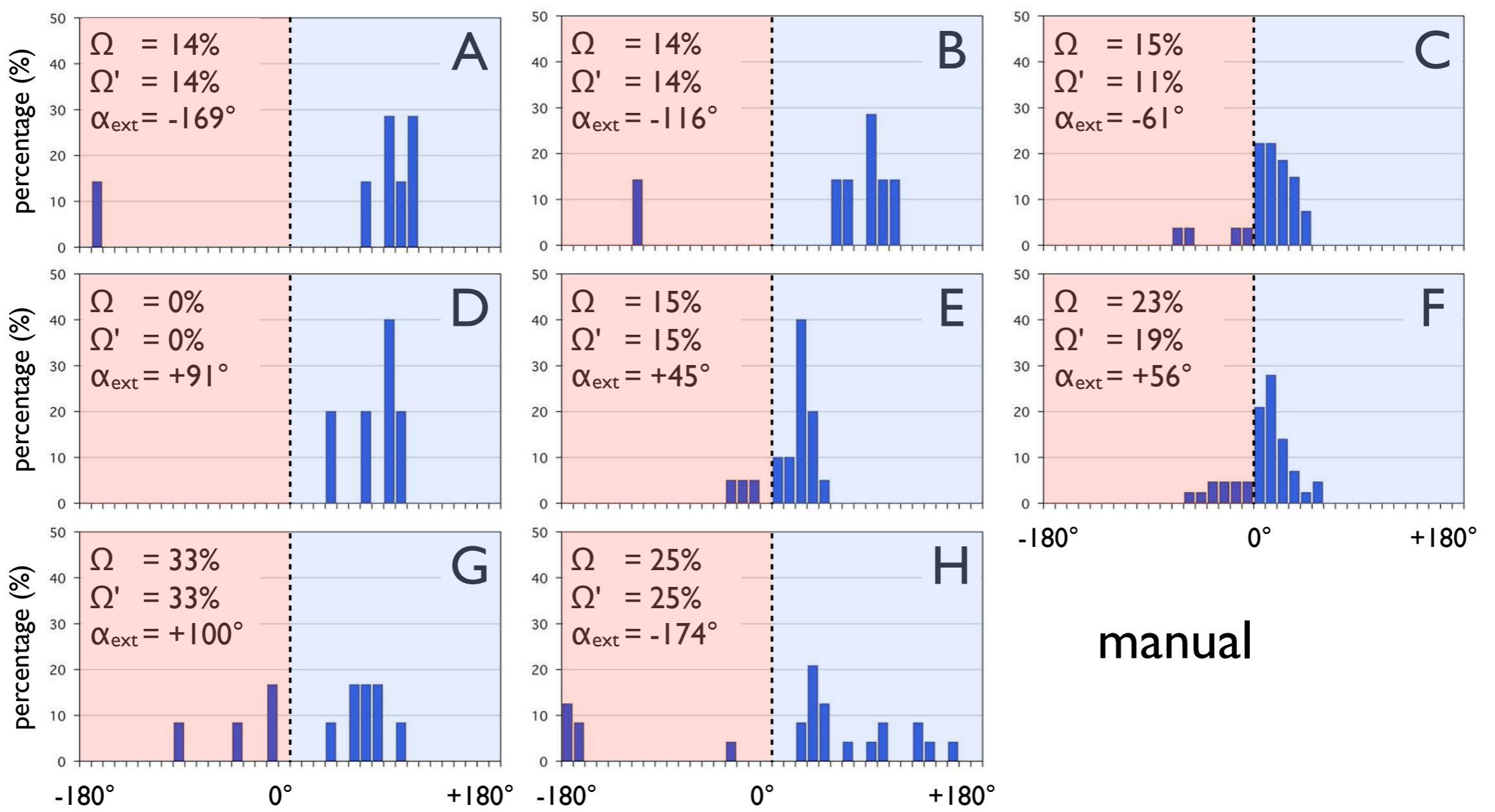
(c) automatically digitized outlines, minimal distance between points = 10 pixels, smoothing error = 0.5 pixel;  
circles mark locations of digitized vertices.





**Figure 17.16**

Shape descriptors of manually and automatically digitized shapes.  
 Outlines are digitized as in Figure 17.15.a (black), 17.15.b (green), 17.15.c (red);  
 L / S = aspect ratio, where L = longest projection, S = shortest projection;  
 SF<sub>1</sub> = P / P<sub>equ</sub> = shape factor I;  
 PARIS = Percentile Average Relative Indented Surface;  
 deltP = excess perimeter;  
 deltA = defect area.



**Figure 17.17**

Descriptors of angularity of manually and automatically digitized shapes. Histograms of vertex angles are shown for test shapes of Figure 17.15:

(a) for manually digitized outlines;

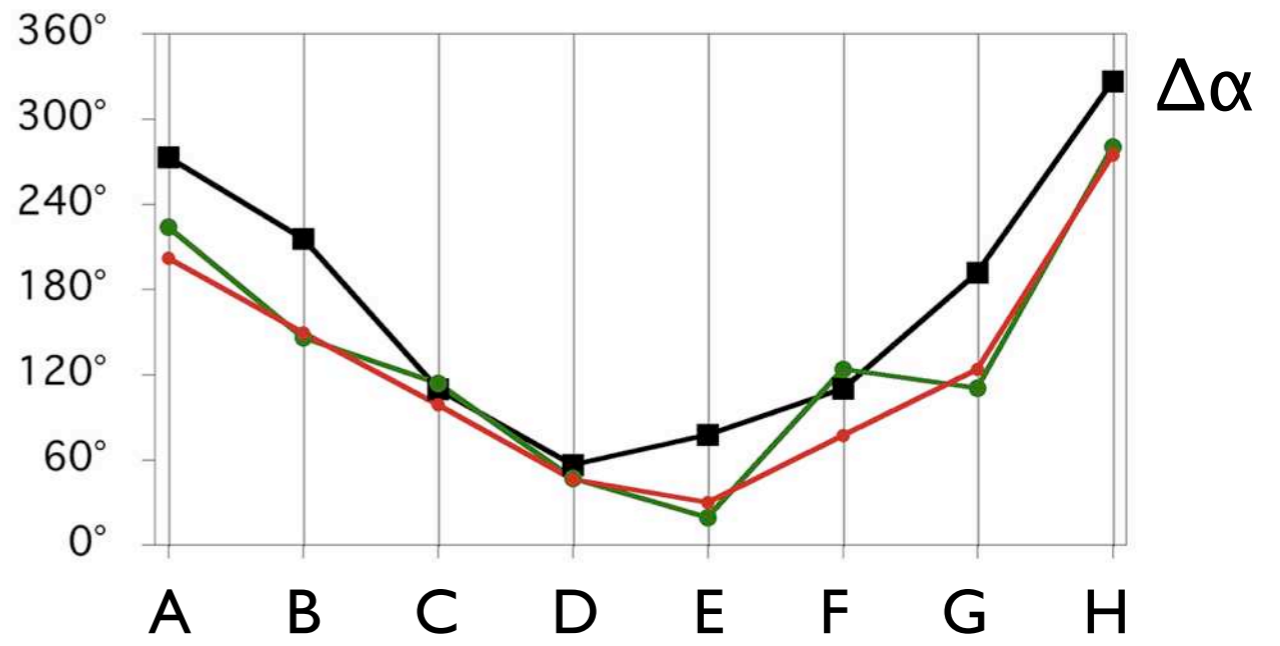
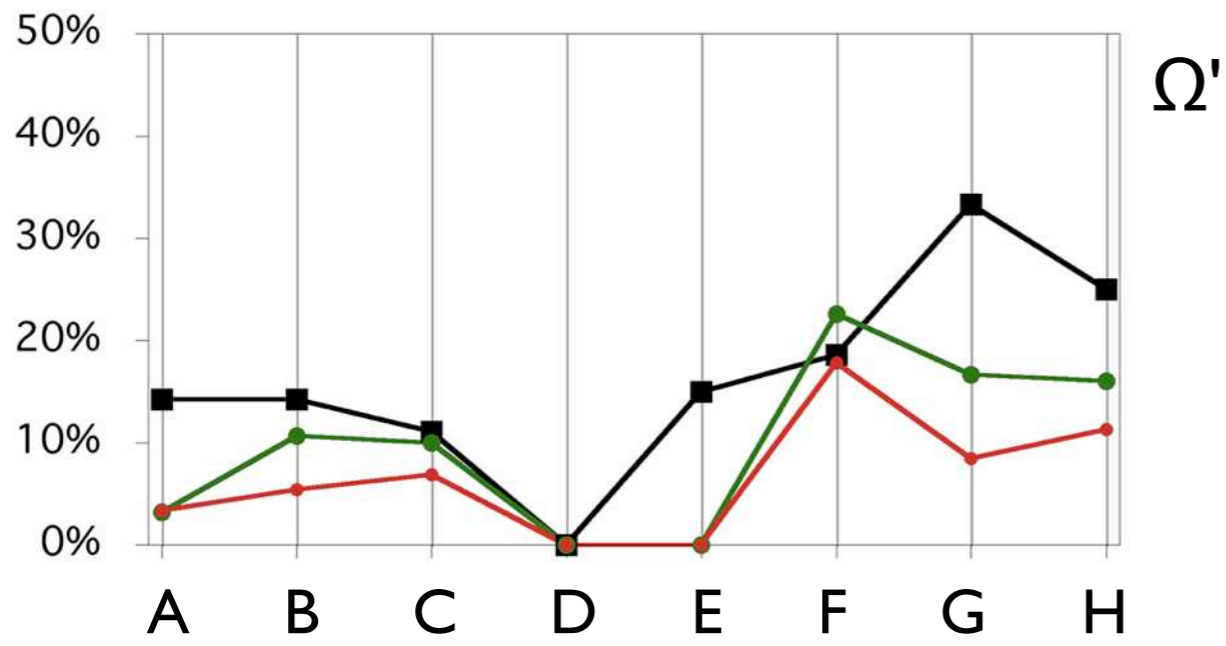
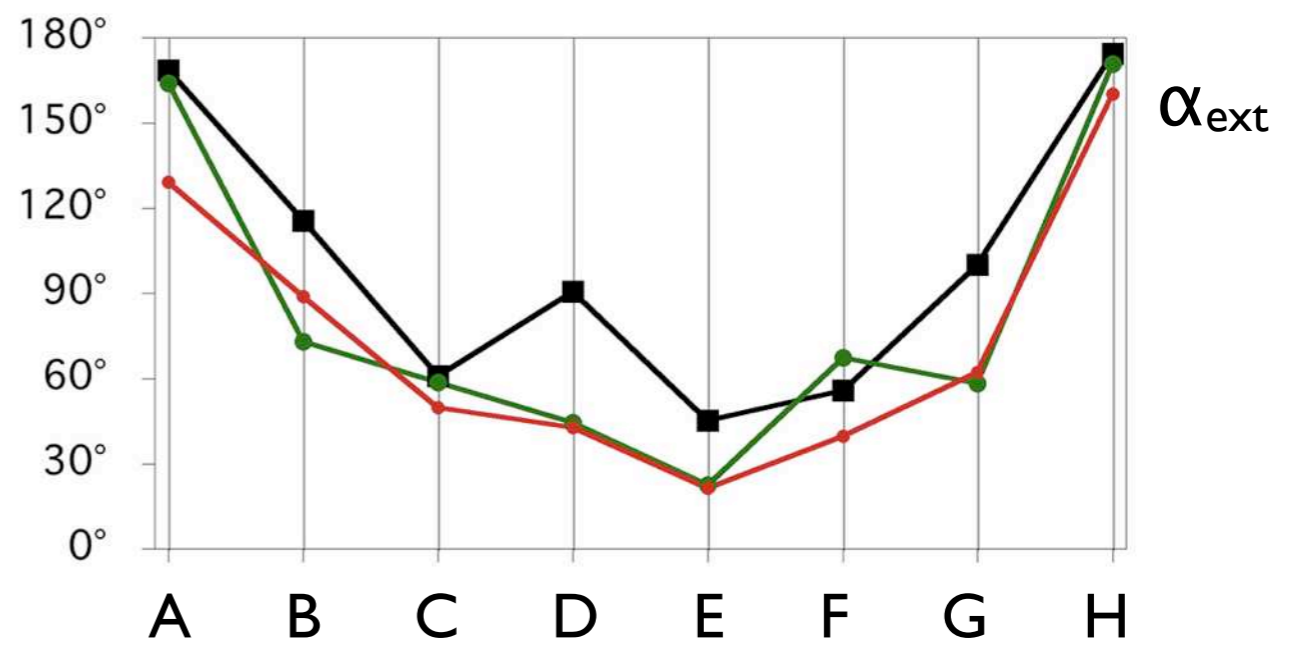
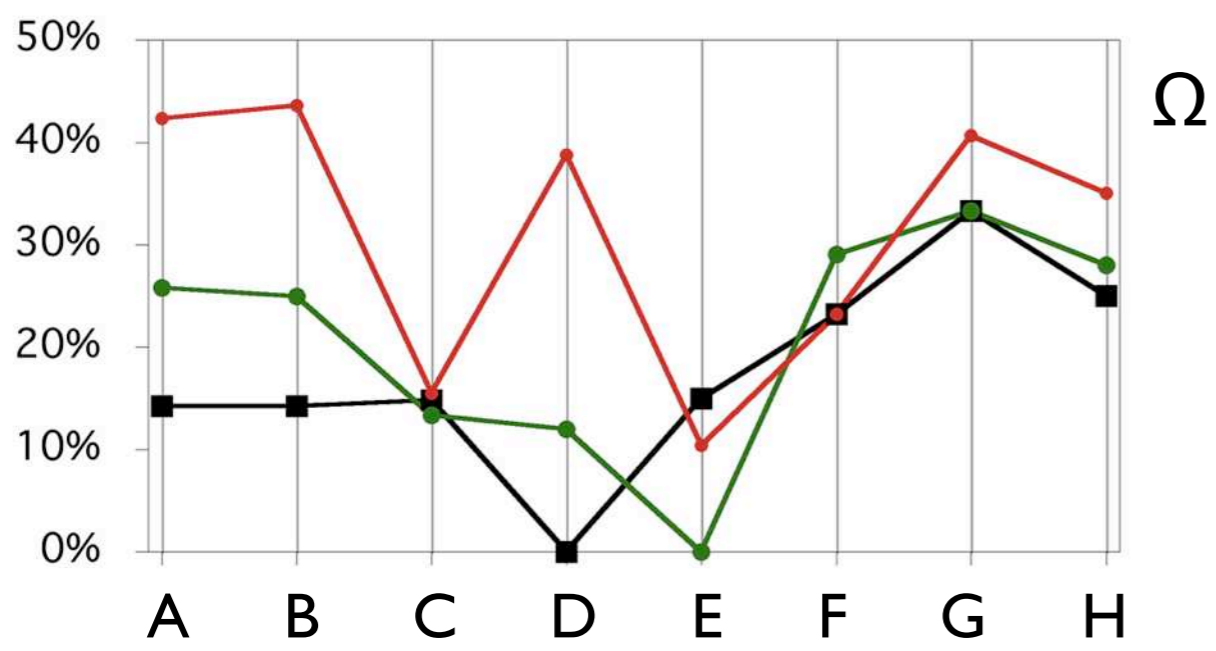
(b) for automatically digitized outlines (wide spacing of vertices);

(c) for automatically digitized outlines (close spacing of vertices);

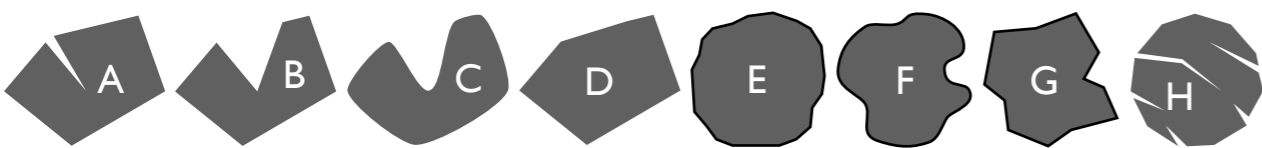
$\Omega$  = sum of frequencies form  $-180^\circ$  to  $0^\circ$ ;

$\Omega'$  = sum of frequencies form  $-180^\circ$  to  $-10^\circ$ ;

$\alpha_{\text{ext}}$  = value of maximum absolute vertex angle.

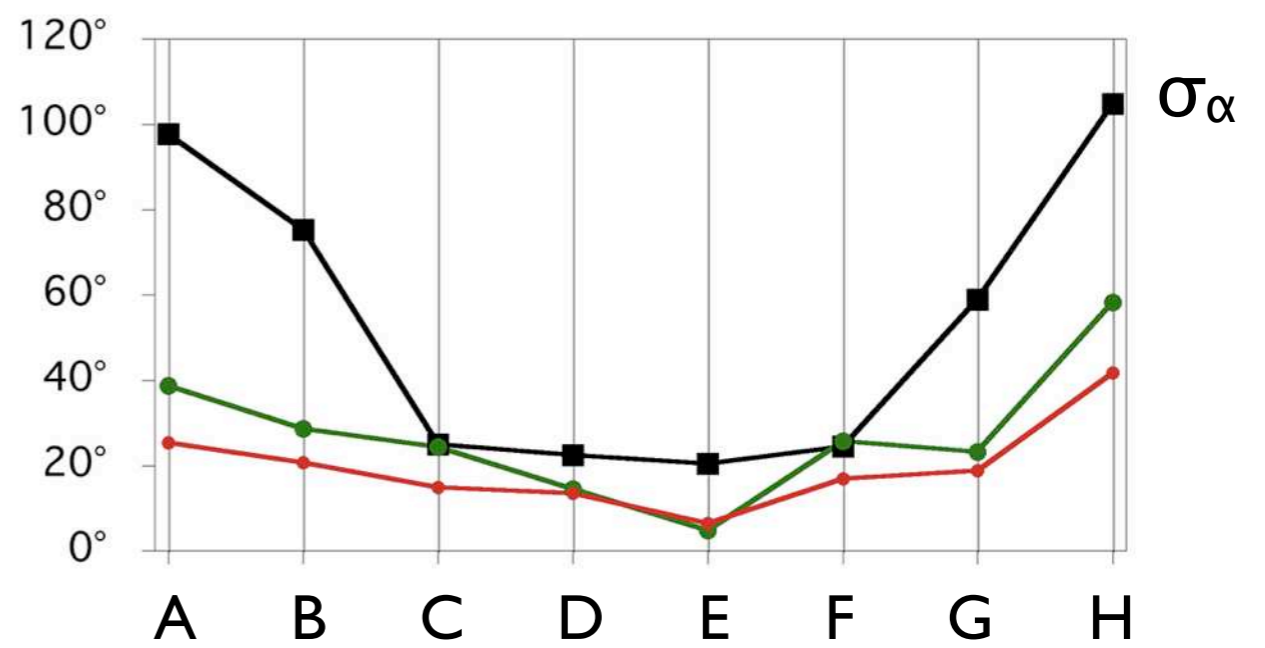


shapes:



mode of digitization:

manual      auto d=10      auto d=20



**Figure 17.18**

Comparison of descriptors of angularity for manual and automatic digitization.

Outlines are digitized as in Figure 17.15.a (black), 17.15.b (green), 17.15.c (red);

$\Omega$  = sum of frequencies form  $-180^\circ$  to  $0^\circ$ ;

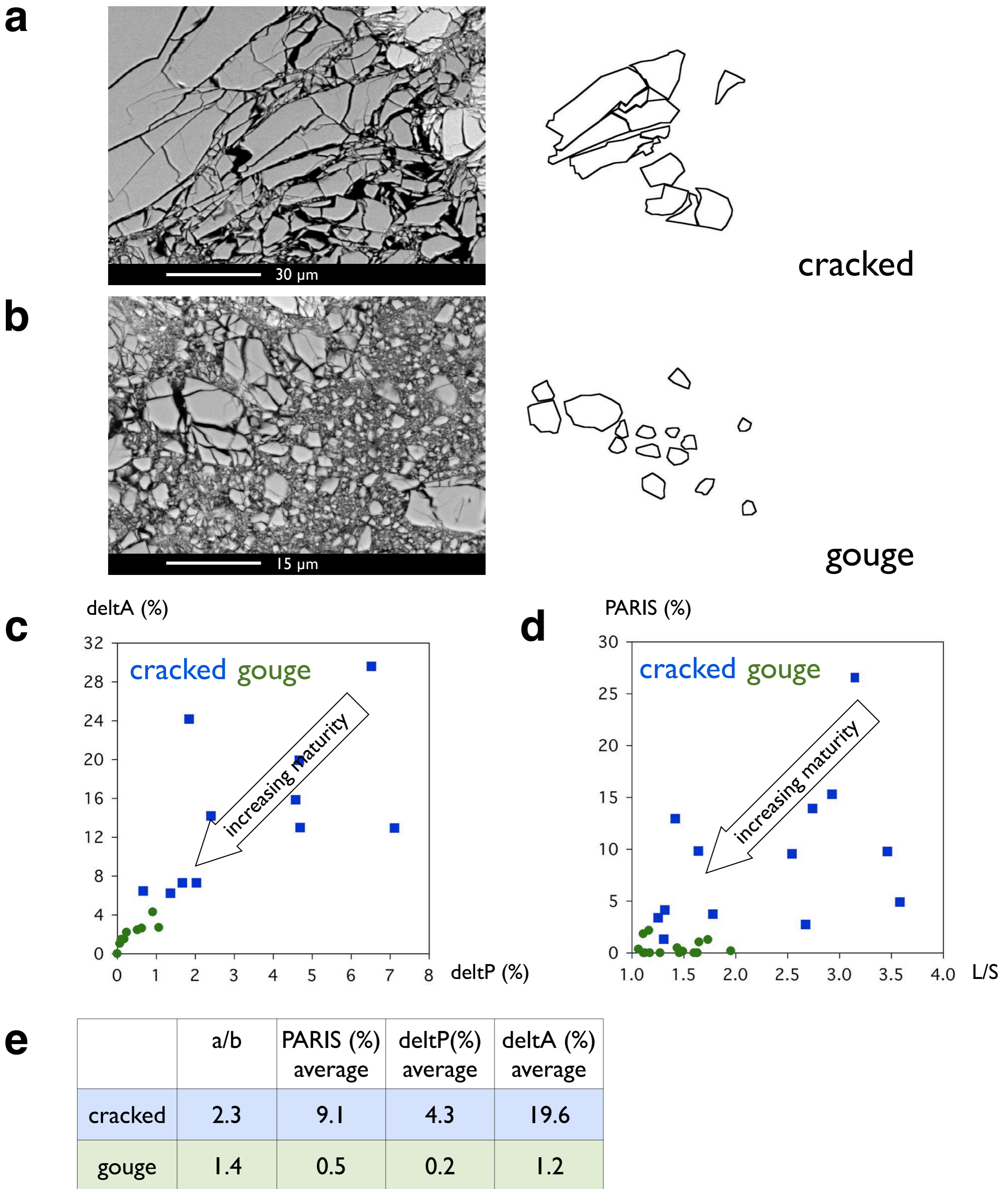
$\Omega'$  = sum of frequencies form  $-180^\circ$  to  $-10^\circ$ ;

$\alpha_{ext}$  = extreme angle = value of maximum absolute vertex angle;

$\Delta\alpha$  = range of angles =  $\alpha_{max} - \alpha_{min}$ ;

$\sigma_\alpha$  = standard deviation of vertex angles.





**Figure 17.19**

Shape analysis of fault rocks.

SEM micrographs (BSE contrast) and digitized outlines

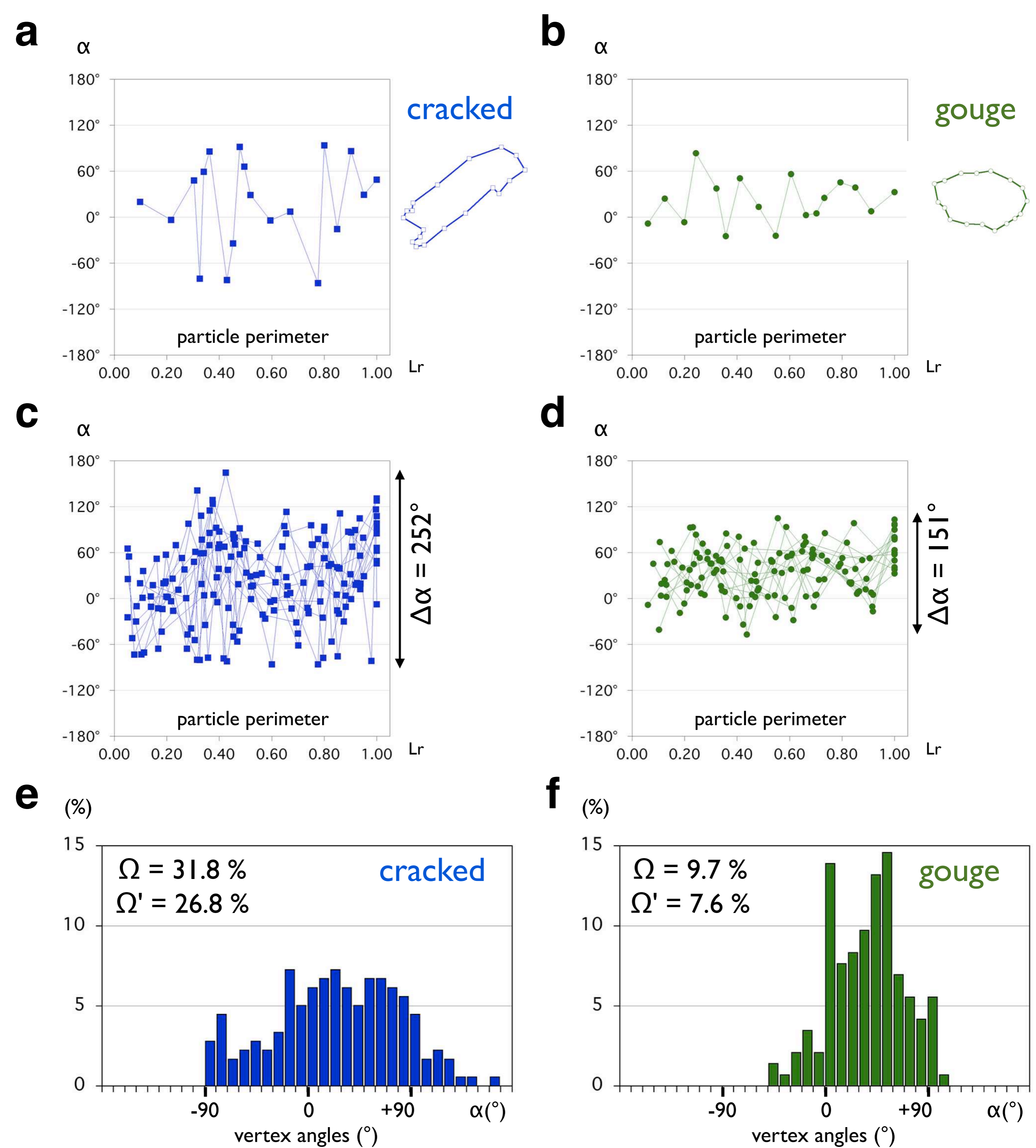
(a) of fragments with angular shapes ('cracked');

(b) of gouge with rounded shapes ('gouge');

(c) plot of 'defect area',  $\Delta A$ , versus 'excess perimeter',  $\Delta P$ ;

(d) plot of PARIS factor versus aspect ratio,  $L/S$ ;

(e) list of average values for (a) and (b).



**Figure 17.20**

Angularity of fault rocks.

The fault rock microstructures shown in Figure 17.19.a and 17.19.b are analyzed.

(a) Vertex angles,  $\alpha$ , along relative length of outline of one particle of 'cracked' microstructure, ( $0 \leq L_r \leq 1.00$ ), shape of particle is shown next to graph;

(b) same as (a) for one 'gouge' particle;

(c) same as (a) for all particles of 'cracked' microstructure;

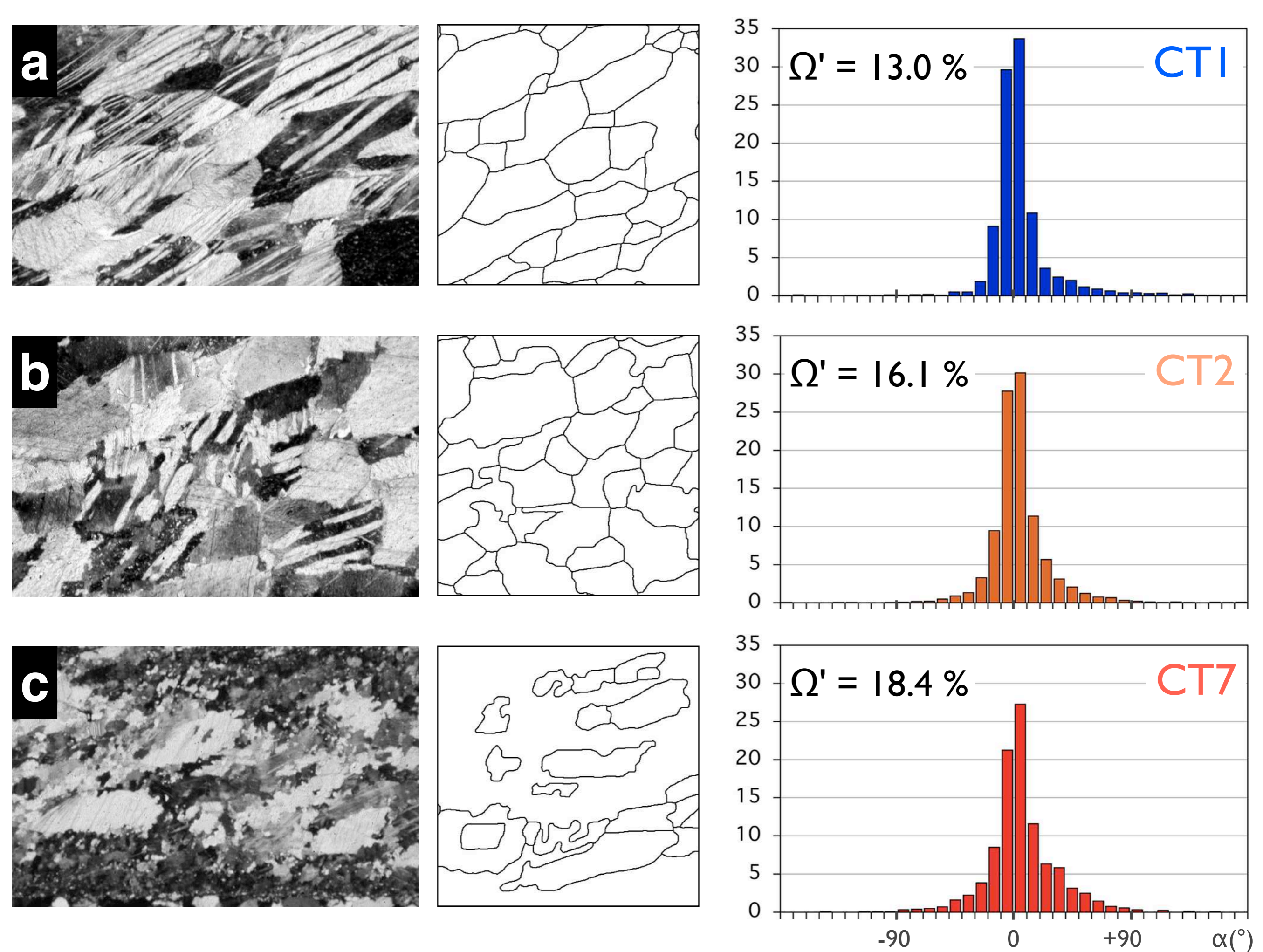
(d) same as (a) for all 'gouge' particles;

(e) histogram of vertex angles of 'cracked';

(f) histogram of vertex angles of 'gouge';

$\Omega$  = fraction of histogram with  $\alpha \leq 0^\circ$ ;  $\Omega'$  = fraction of histogram with  $\alpha \leq -10^\circ$ .





**Figure 17.21**

Shape analysis of dynamically recrystallized marble.

Samples are from Schmid et al. (1987).

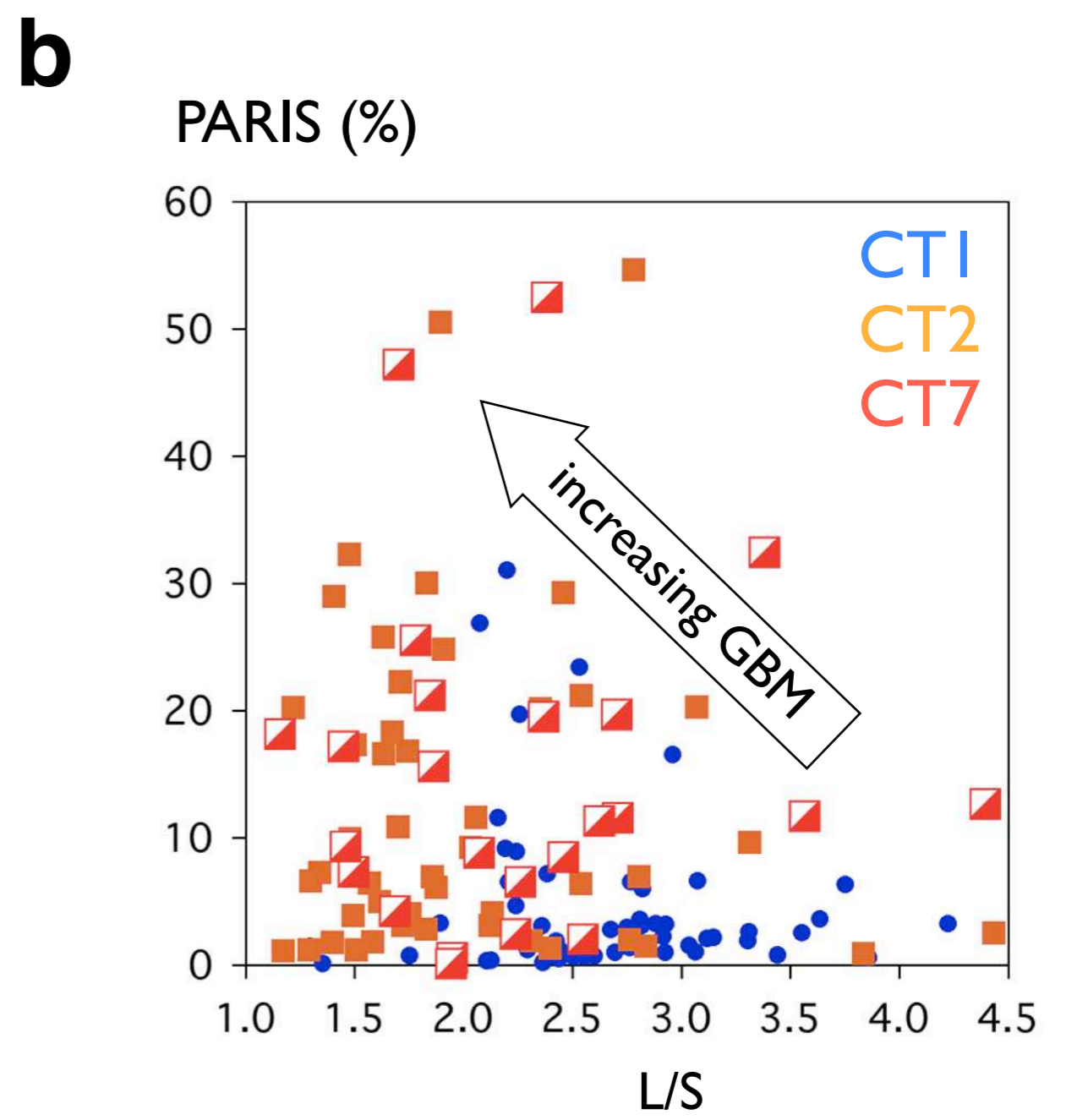
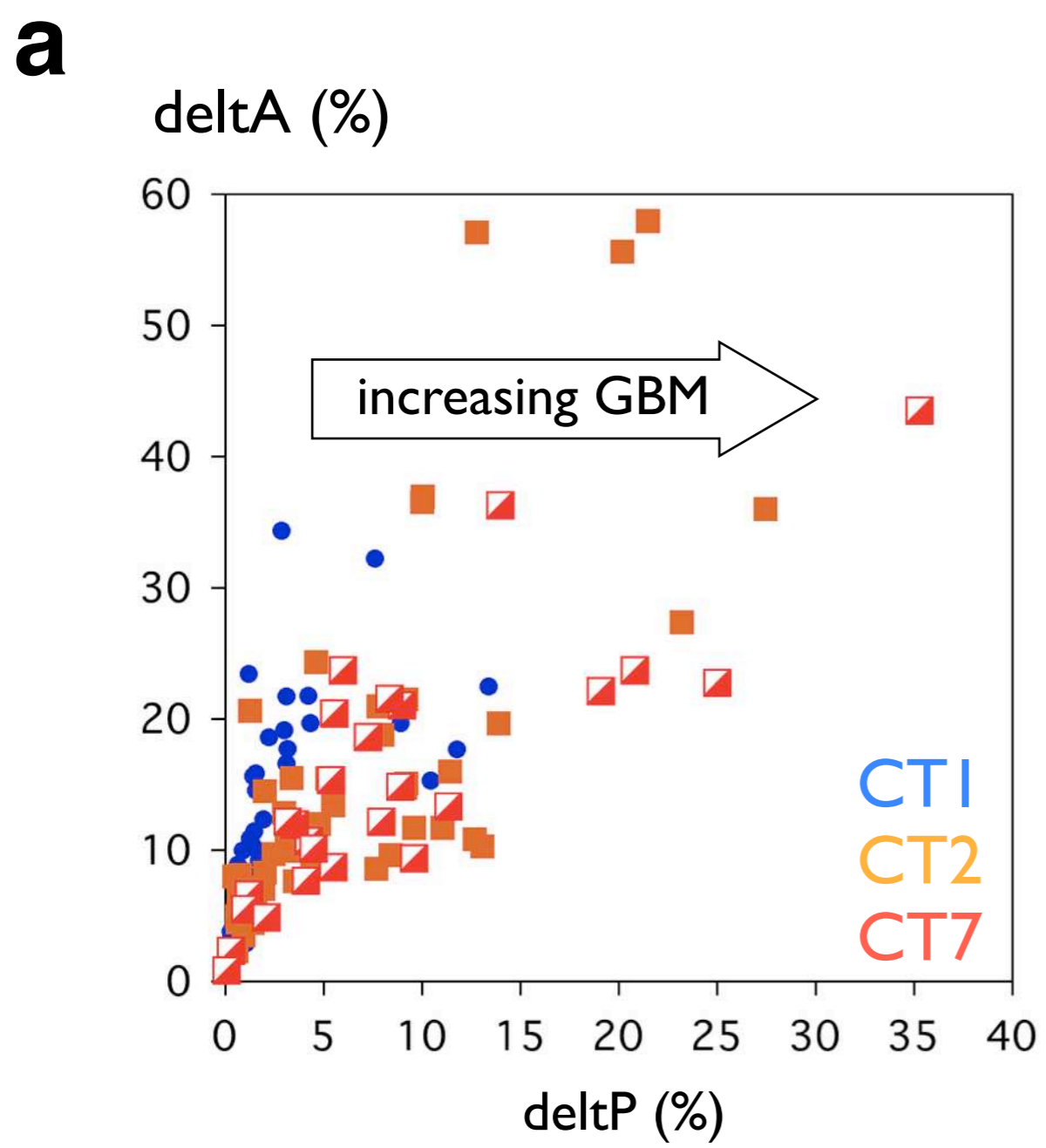
From left to right, micrographs (ultrathin section, crossed polarizers), digitized outlines and histograms of vertex angles are shown for:

(a) CT1, deformed at 600°C;

(b) CT2, deformed at 800°C to low strain ( $\gamma < 1$ );

(c) CT7, deformed at 800°C to moderate strain ( $\gamma \sim 2.5$ ).

$\Omega'$  = fraction of histogram with  $\alpha \leq -10^\circ$ .

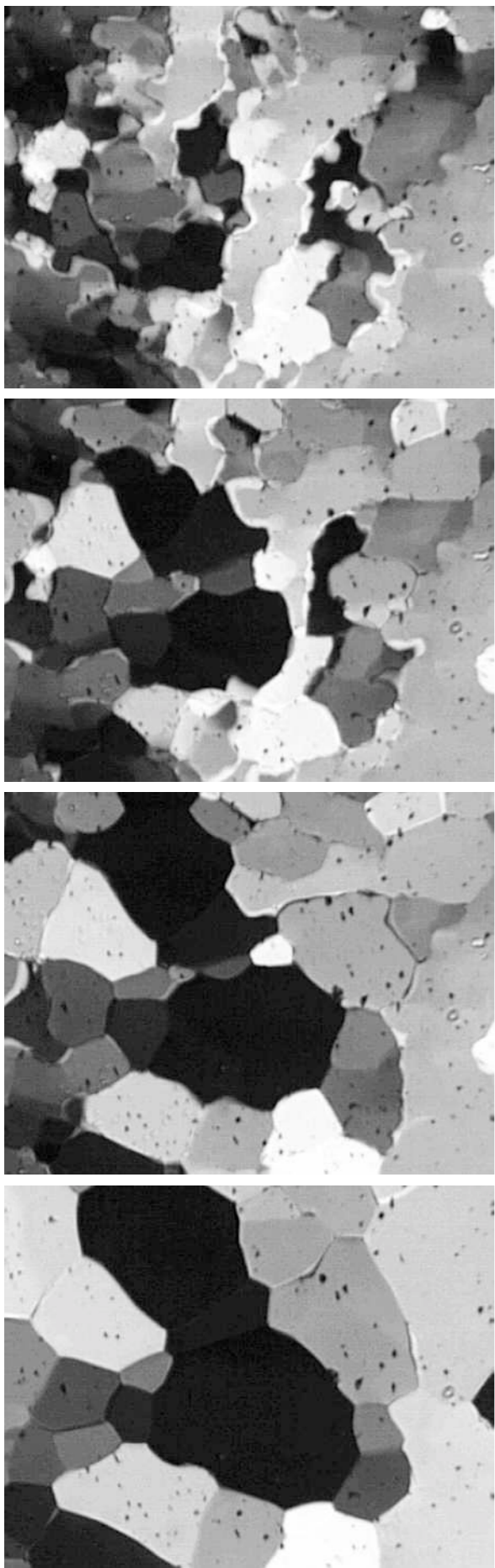
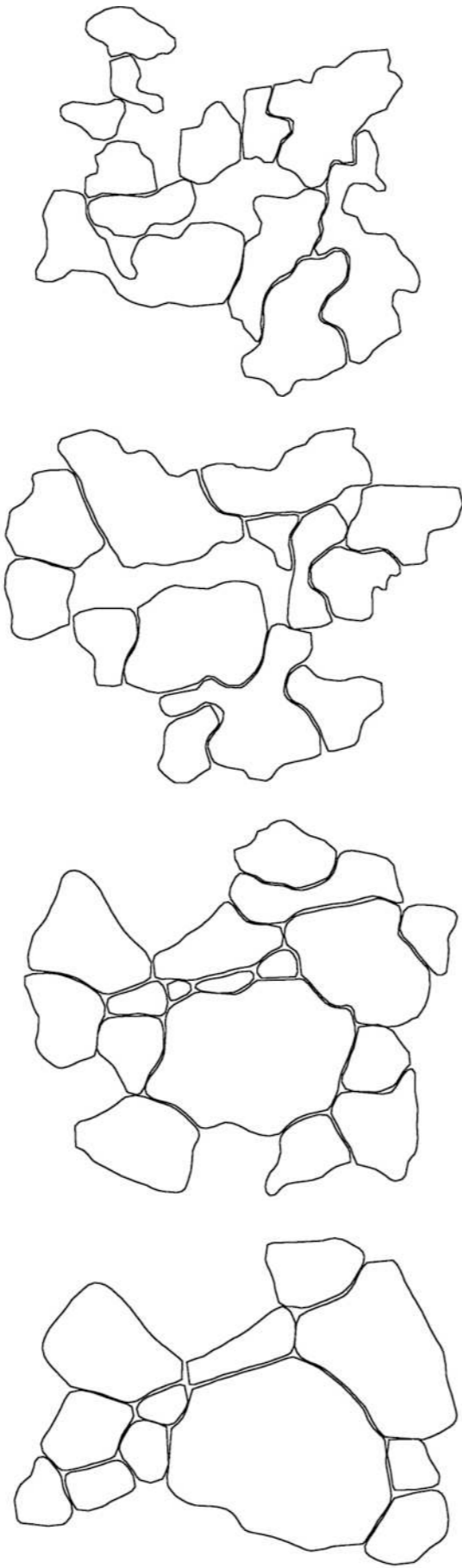
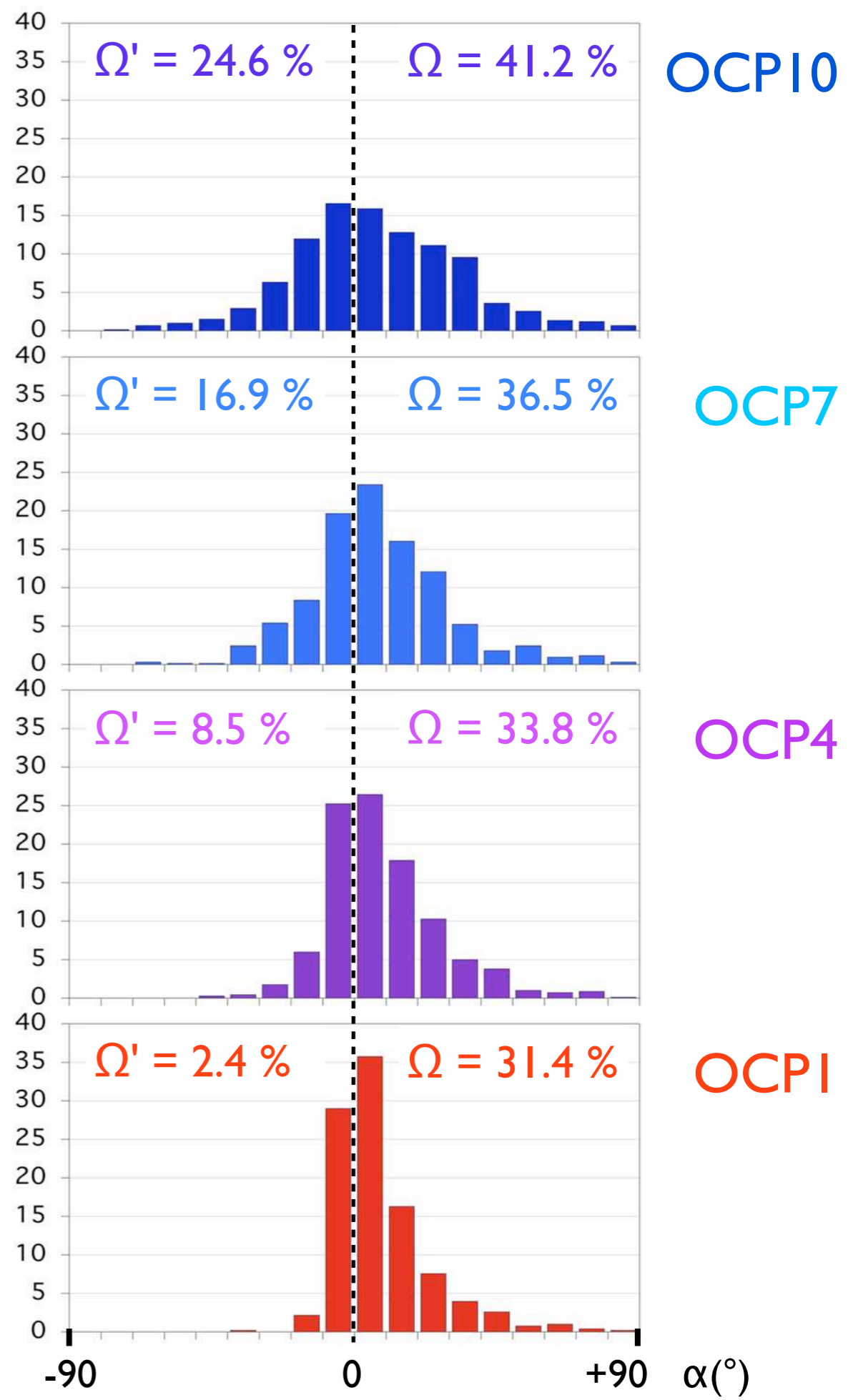


**c**

	L/S average	PARIS (%) average	deltP(%) average	deltA (%) average
CT1	2.65	4.9	2.3	10.7
CT2	2.00	15.0	6.5	15.8
CT7	2.20	20.9	8.6	15.4

**Figure 17.22**  
Effect of grain boundary migration on grain shape.  
Evaluation of microstructures shown in Figure 17.21.  
(a) Plot of 'defect area', deltA, versus 'excess perimeter', deltP;  
(b) plot of PARIS factor versus aspect ratio, L/S;  
(c) list of average values for CT1, CT2, and CT7.



**a****b****c****Figure 17.23**

Effect of annealing on angularity.

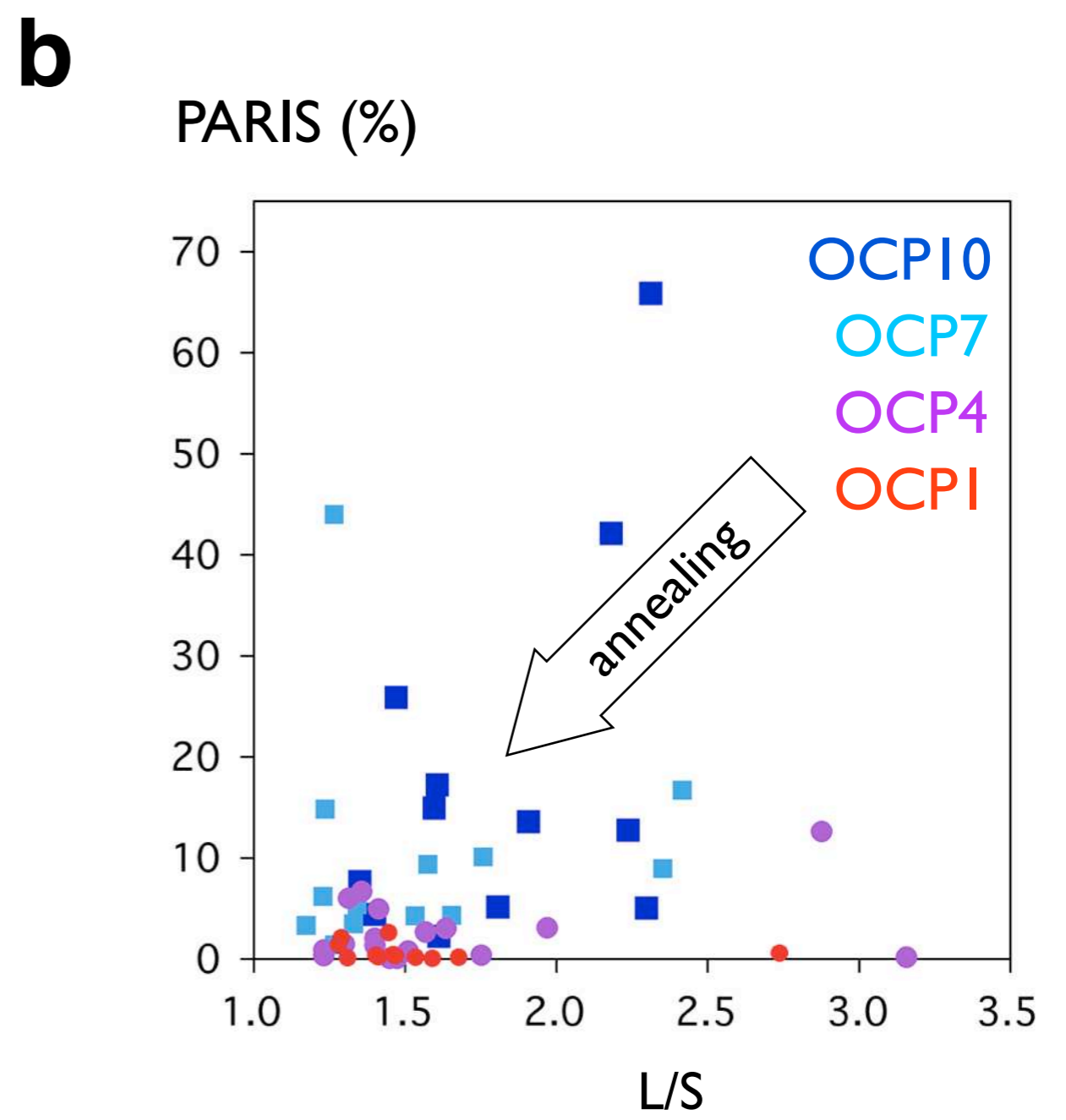
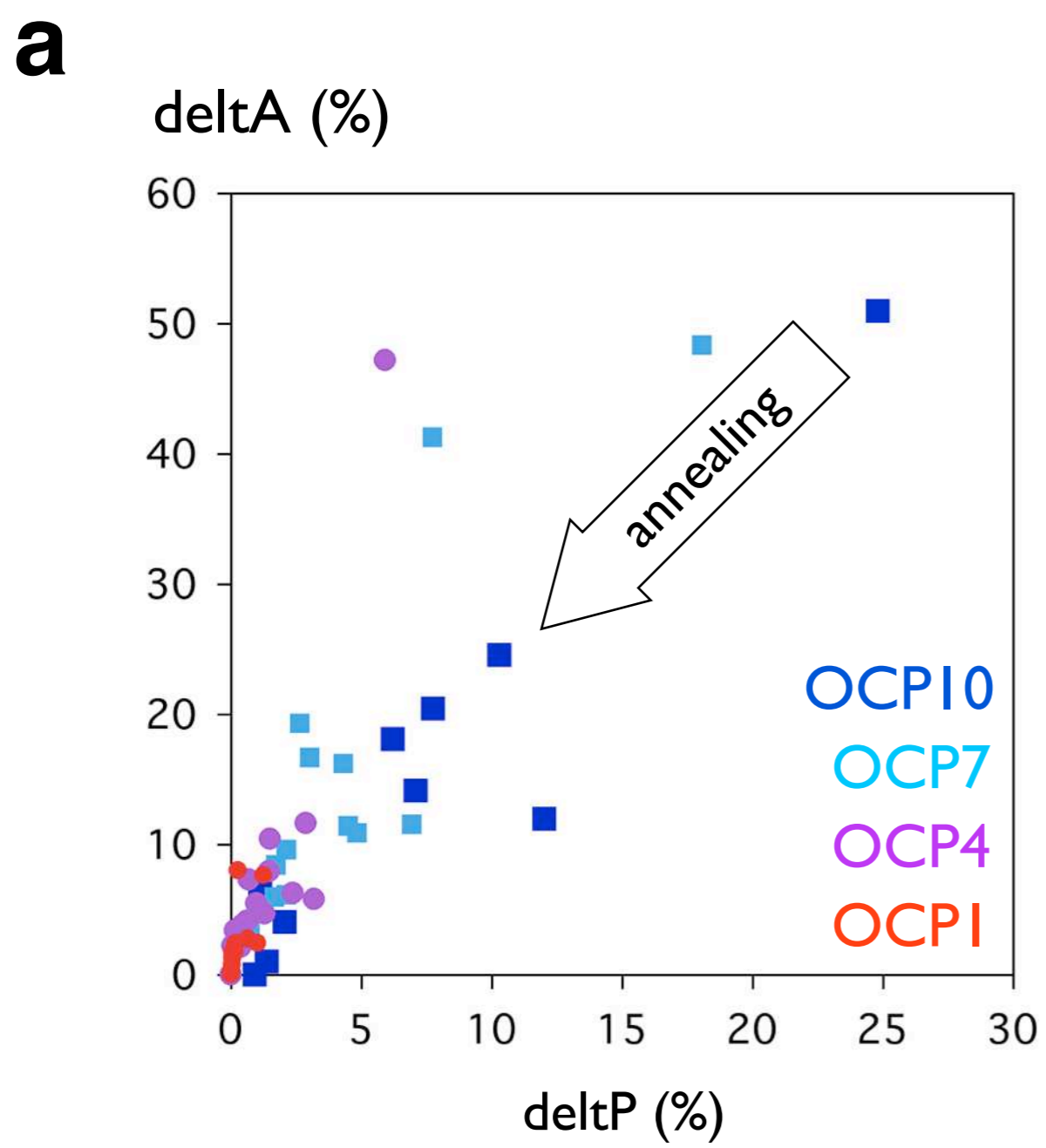
Four stages of annealing of dynamically recrystallized Octochloropropane ('see-through' experiment by Youngdo Park, Jin-Han Ree, images courtesy Wynn Means).

(a) Optical micrographs, crossed polarizers;

(b) digitized outlines;

(c) histograms of vertex angles;

 $\Omega$  = fraction of histogram with  $\alpha < 0^\circ$ ;  $\Omega'$  = fraction of histogram with  $\alpha \leq -10^\circ$ .



**c**

	L/S average	PARIS (%) average	deltP(%) average	deltA (%) average
OCPI0	1.81	18.10	7.75	20.50
OCP7	1.55	10.20	4.63	16.15
OCP4	1.65	2.69	1.30	7.31
OCPI	1.55	0.66	0.33	2.57

**Figure 17.24**

Effect of annealing on grain shape.

Evaluation of microstructures shown in Figure 17.23.

(a) Plot of 'defect area',  $\text{deltA}$ , versus 'excess perimeter',  $\text{deltP}$ ;

(b) plot of PARIS factor versus aspect ratio,  $L/S$ ;

(c) list of average values for OCPI0 (dynamically recrystallized) to OCPI (annealed).